AMERICAN SOCIETY FOR MICROBIOLOGY | Journal of Virology®

VIRUS-CELL INTERACTIONS

# Interplay of PA-X and NS1 Proteins in Replication and Pathogenesis of a Temperature-Sensitive 2009 Pandemic H1N1 Influenza A Virus

**Aitor Nogales,[a] Laura Rodriguez,[a] Marta L. DeDiego,[a,b] David J. Topham,[a,b] Luis Martínez-Sobrido[a]**

Department of Microbiology and Immunology[a] and David Smith Center for Immunology and Vaccine Biology,[b] University of Rochester, Rochester, New York, USA

**ABSTRACT** Influenza A viruses (IAVs) cause seasonal epidemics and occasional pandemics, representing a serious public health concern. It has been described that one mechanism used by some IAV strains to escape the host innate immune responses and modulate virus pathogenicity involves the ability of the PA-X and NS1 proteins to inhibit the host protein synthesis in infected cells. It was reported that for the 2009 pandemic H1N1 IAV (pH1N1) only the PA-X protein had this inhibiting capability, while the NS1 protein did not. In this work, we have evaluated, for the first time, the combined effect of PA-X- and NS1-mediated inhibition of general gene expression on virus pathogenesis, using a temperature-sensitive, live-attenuated 2009 pandemic H1N1 IAV (pH1N1 LAIV). We found that viruses containing PA-X and NS1 proteins that simultaneously have ($PA_{WT}^{+}$/$NS1_{MUT}^{+}$) or do not have ($PA_{MUT}^{-}$/$NS1_{WT}^{-}$) the ability to block host gene expression showed reduced pathogenicity *in vivo*. However, a virus where the ability to inhibit host protein expression was switched between PA-X and NS1 ($PA_{MUT}^{-}$/$NS1_{MUT}^{+}$) presented pathogenicity similar to that of a virus containing both wild-type proteins ($PA_{WT}^{+}$/$NS1_{WT}^{-}$). Our findings suggest that inhibition of host protein expression is subject to a strict balance, which can determine the successful progression of IAV infection. Importantly, knowledge obtained from our studies could be used for the development of new and more effective vaccine approaches against IAV.

**IMPORTANCE** Influenza A viruses (IAVs) are one of the most common causes of respiratory infections in humans, resulting in thousands of deaths annually. Furthermore, IAVs can cause unpredictable pandemics of great consequence when viruses not previously circulating in humans are introduced into humans. The defense machinery provided by the host innate immune system limits IAV replication; however, to counteract host antiviral activities, IAVs have developed different inhibition mechanisms, including prevention of host gene expression mediated by the viral PA-X and NS1 proteins. Here, we provide evidence demonstrating that optimal control of host protein synthesis by IAV PA-X and/or NS1 proteins is required for efficient IAV replication in the host. Moreover, we demonstrate the feasibility of genetically controlling the ability of IAV PA-X and NS1 proteins to inhibit host immune responses, providing an approach to develop more effective vaccines to combat disease caused by this important respiratory pathogen.

**KEYWORDS** host response, influenza, influenza vaccines, virus-host interactions

**Received** 28 April 2017 **Accepted** 11 June 2017

**Accepted manuscript posted online** 21 June 2017

**Citation** Nogales A, Rodriguez L, DeDiego ML, Topham DJ, Martínez-Sobrido L. 2017. Interplay of PA-X and NS1 proteins in replication and pathogenesis of a temperature-sensitive 2009 pandemic H1N1 influenza A virus. J Virol 91:e00720-17. https://doi.org/10.1128/JVI.00720-17.

**Editor** Stacey Schultz-Cherry, St. Jude Children's Research Hospital



Address correspondence to Luis Martínez-Sobrido, luis_martinez@urmc.rochester.edu.

Influenza A viruses (IAVs) are enveloped viruses that belong to the *Orthomyxoviridae* family and contain a genome that comprises eight single-stranded negative-sense RNA segments that encode 10 to 14 proteins (1). The RNA-dependent RNA polymerase

(RdRp) of IAV is a heterotrimeric complex consisting of the polymerase basic 1 and 2 (PB1 and PB2) and polymerase acidic (PA) proteins, which together with the viral nucleoprotein (NP) are the minimal components required for viral genome replication and gene transcription (2). In mammals, IAV is a respiratory pathogen that first infects the upper respiratory tract and may lead to pathology when replication moves to the lower respiratory tract (3). The temperature gradient between these two airways has allowed the development of cold-adapted (*ca*), temperature-sensitive (*ts*), live-attenuated (*att*) influenza viruses that replicate efficiently in the cooler upper respiratory tract but cannot damage the lower respiratory tract because the warmer temperature restricts viral replication (4). This principle has been used to generate safe live-attenuated influenza vaccines (LAIVs) with high protection efficacy, mediated mainly by the humoral and cellular responses induced upon vaccination. For IAVs, these *ca*, *ts*, and *att* properties have been mapped to five amino acid residues located in the viral replication complex (PB2, N265S; PB1, K391E, D581G, and A661T; NP, D34G) of A/Ann Arbor/6/60 H2N2 (A/AA/6/60) (5, 6). The attenuation mechanisms are not totally understood but could involve several steps in the replication cycle of the virus (4). Importantly, when the *ts* signature of A/AA/6/60 was introduced into three different viruses (influenza virus A/Puerto Rico/8/34 H1N1 [PR8] [7, 8], canine influenza virus H3N8 [9, 10], or pandemic influenza virus A/New York/1682/2009 H1N1 [11]), a similar *ts* viral phenotype was observed in tissue culture cells and in mouse models of infection. Moreover, *ca*, *ts*, and *att* viruses have been previously utilized to evaluate additional mutations that can increase the safety profile of a vaccine candidate (7, 11).

Defense strategies provided by the innate immune system limit IAV replication (12), so IAVs have to counteract host antiviral activities, especially the production of interferon (IFN) and the activities of IFN-induced gene (ISG) proteins that inhibit virus replication (13, 14). It was recently reported that segment 3 of IAV encodes the PA protein but also a second protein, PA-X, which is translated as a +1 frameshift open reading frame (ORF) within the PA viral segment (15). During the frameshift, PA-X incorporates the first N-terminal 191 amino acids of the PA protein with a short C-terminal sequence (either 61 or 41 codons) from the alternative translation (15). Multiple functions have been attributed to PA-X, including degradation of host mRNA that leads to inhibition of host protein synthesis and contributes to blocking the cellular antiviral responses (15–19). Moreover, the PA-X protein has been shown to be involved in modulating host inflammation, the immune response, and apoptosis (15, 17, 20–22). Although PA and PA-X have the same N-terminal domain, PA-X has a much stronger endonucleolytic activity, indicating that the C-terminal region is responsible for the inhibition of the host protein expression (23).

The other prevalent IAV antiviral protein is the nonstructural protein 1 (NS1), which is the primary transcript produced from the viral genome segment 8 (NS) (14). NS1 is a multifunctional protein (14) that mainly counteracts the host innate immune responses by multiple mechanisms, allowing the virus to efficiently replicate in IFN-competent systems (24–27). Moreover, NS1 has the ability to inhibit host gene expression, including preventing upregulation of ISGs with antiviral activity (14, 26, 28–30). For that, the NS1 proteins from some IAV strains bind to the 30-kDa subunit of the cleavage and polyadenylation specificity factor (CPSF30), blocking the processing of cellular mRNAs (25, 31–33). However, the 2009 pandemic H1N1 IAV (pH1N1) NS1 has been shown to lack CPSF30 binding ability and therefore does not block host gene expression, a property that could be restored by introduction of amino acid changes R108K, E125D, and G189D (34). Interestingly, a recombinant pH1N1 expressing an NS1 with these substitutions, which could inhibit host gene expression, was more efficient than the wild-type (WT) virus in antagonizing the host innate immune response. However, *in vivo*, the NS1 mutant pH1N1 virus grew to lower titers in mouse lungs and was slightly less pathogenic (34).

Although the independent role of IAV PA-X and NS1 proteins in virulence has been investigated previously, here we evaluated, for the first time, the impact of the interplay between these two proteins in virus replication, pathogenesis, and regulation of innate

and adaptive immune responses both *in vitro* and *in vivo*. To carry out this study, we have generated a *ca*, *ts*, and *att* A/California/4_NYICE_E3/2009 H1N1 strain (referred to here as pH1N1 LAIV virus) that provides three advantages: safety, sensitivity, and potential as a vaccine candidate. First, because a recombinant pH1N1 harboring inhibitory PA-X and NS1 proteins could lead to a more virulent virus (35–38), we selected, for safety reasons, to use the *ca*, *ts*, and *att* pH1N1 LAIV virus. Second, we and others have previously shown that LAIVs provide a more sensitive approach to study mutations affecting overall viral replication and pathogenicity (5, 7, 9–11, 39). Finally, the results obtained from our studies could be used to identify and develop more efficient LAIV candidates with acceptable safety profiles by modulating the virus' ability to control the host immune responses (7, 11). Finding new LAIV candidates is important because the effectiveness of the current (2012) quadrivalent LAIV has been shown to be low, attributed mainly to the H1N1 IAV component. Based on its low effectiveness, the Advisory Committee on Immunization Practices (ACIP) recommended that the quadrivalent LAIV should not be used (40, 41).

Our studies indicate that viruses simultaneously encoding PA-X and NS1 proteins that are either able ($PA_{WT}^{+}/NS1_{MUT}^{+}$) or unable ($PA_{MUT}^{-}/NS1_{WT}^{-}$) to block the host gene expression are highly attenuated *in vivo*. In contrast, viruses in which only one of the viral PA-X or NS1 proteins (i.e., $PA_{WT}^{+}/NS1_{WT}^{-}$ or $PA_{MUT}^{-}/NS1_{MUT}^{+}$) is able to inhibit host gene expression were less attenuated and better able to induce both innate and adaptive immune responses *in vivo*. Altogether, these results suggest that inhibition of host gene expression depends on a strict balance between the NS1 and PA-X proteins. These results further demonstrate the feasibility of modifying the ability of IAV PA-X and NS1 proteins to inhibit host immune responses for the development of more effective vaccine approaches to prevent influenza viral infections.

## RESULTS

**Generation and characterization of a recombinant pH1N1 LAIV virus.** In order to generate a pH1N1 LAIV virus, we introduced four *ts* mutations identified in previous studies into the PB2 (N265S) and PB1 (K391E, D581G, and A661T) ORFs of pH1N1 (Fig. 1A) (7, 9, 10, 39). No mutation was introduced into the viral NP, since pH1N1 NP already contains a G at position 34. To confirm that the introduced mutations confer a *ts* phenotype to the pH1N1 polymerase complex, we first performed a minigenome (MG) assay at different temperatures (Fig. 1B). Both combinations of plasmids (WT and LAIV) resulted in similar *Gaussia* luciferase (Gluc) expression levels at 33°C; however, Gluc expression was significantly reduced at higher temperatures (37°C and 39°C) in cells transfected with the pH1N1 LAIV plasmids, consistent with previous results shown for other IAV LAIV strains (9–11). Importantly, Western blot analysis shows similar levels of NP expression at each temperature for WT- and LAIV-transfected cells (Fig. 1C).

Next, we generated a pH1N1 LAIV virus and evaluated viral replication in a multicycle growth kinetic study at different temperatures (33°C, 37°C, and 39°C) and compared the results to those for the pH1N1 WT virus (Fig. 2A). To that end, MDCK cells were infected at a low multiplicity of infection (MOI) (0.001), and viral titers in tissue culture supernatants (TCS) were determined at the indicated times postinfection (p.i.). At 33°C, pH1N1 WT and LAIV viruses reached similar titers at the peak of infection (48 to 72 h). However, at higher temperatures (37°C and particularly 39°C), pH1N1 WT replicated at higher titers than pH1N1 LAIV. The *ts* phenotype of the pH1N1 LAIV virus was further confirmed by plaque assay (Fig. 2B). As expected, the lysis plaques produced by the pH1N1 LAIV virus were slightly smaller than those produced by pH1N1 WT at 37°C. Notably, these differences were more pronounced at 39°C, where only point plaques were observed for the pH1N1 LAIV virus. These results demonstrate that mutations introduced in PB2 and PB1 conferred a *ts* phenotype to pH1N1, as previously described for other influenza viruses (4, 5, 7–11).

**Interplay of effects of pH1N1 PA-X and NS1 on host gene expression.** PA-X expression occurs from a ribosomal frameshift to the +1 frame at a very conserved sequence (UCC UUU CGU) that overlaps with the PA ORF (Fig. 3A). Several studies have

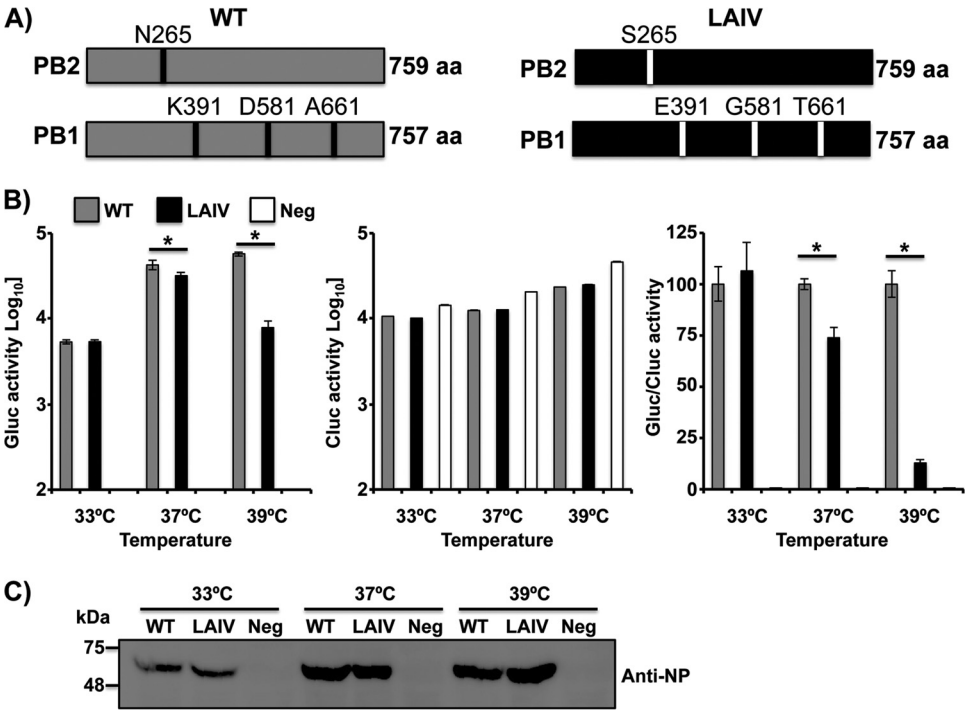


**FIG 1** Effect of temperature on the polymerase activity of the pH1N1 LAIV virus. (A) Schematic representation of PB2 and PB1 viral segments. pH1N1 PB2 and PB1 WT (gray, top) segments with the residues mutated to generate the LAIV virus (black, bottom) are indicated. Numbers on the right signify the amino acid (aa) length of the PB2 and PB1 proteins. (B) Viral replication and transcription. Human 293T cells were transiently cotransfected, using LPF2000, with the pH1N1 WT (gray bars) or LAIV (black bars) ambisense pDZ expression plasmids encoding the minimal requirements for viral genome replication and gene transcription (PB2, PB1, and PA) and NP, together with a vRNA-like expression plasmid encoding Gluc under the control of the human polymerase I promoter (hpPol-I Gluc) and the SV40-Cluc plasmid to normalize transfection efficiencies. At 6 h p.t., cells were placed at 33°C, 37°C, or 39°C, and viral replication and transcription were evaluated at 24 h by luminescence. Gluc (left) and Cluc (middle) activity are represented. Gluc activity was normalized to that of Cluc, and the data were represented as relative activity considering the activity of pH1N1 WT at each indicated temperature as 100% (right). Data represent the means and SDs of the results determined from triplicate wells. *, $P < 0.05$ (WT versus LAIV) using Student's *t* test ($n = 3$ per time point) from Microsoft Excel. (C) NP protein expression levels from cell lysates were evaluated by Western blotting using a specific monoclonal antibody against the viral NP. Sizes of molecular markers are noted on the left.

reported that the PA-X protein is involved in the inhibition of host protein expression (15, 16, 18, 20, 35, 42, 43). In order to generate a PA-X-deficient construct, the frameshift sequence was changed to two different sequences to potentially inhibit PA-X expression (UCC UUC AGA or AGC UUC AGA) (Fig. 3A) (15, 16, 18, 20, 35, 42, 43). Importantly, none of the approaches used for the abolition of the ribosomal frameshift motif changed the PA amino acid sequence. First, we evaluated the effect of each of these strategies on the inhibition of host protein expression (Fig. 4A to C). To this end, human 293T cells were cotransfected with pCAGGS plasmids expressing green fluorescent protein (GFP) and Gluc together with pDZ plasmids encoding the different PA constructs ($PA_{WT}$, $PA_{PMUT}$, or $PA_{MUT}$) or with empty plasmid as control. At 24 h posttransfection (p.t.), GFP expression was evaluated using fluorescence microscopy (Fig. 4A), and Gluc expression levels were quantified in a LumiCount luminometer (Fig. 4B). As expected, based on previous data (35, 43), $PA_{WT}$ blocked the expression of both reporter genes (Fig. 4A and B). However, whereas the $PA_{PMUT}$ construct still inhibited reporter protein expression (both GFP and Gluc) at similar levels as $PA_{WT}$, $PA_{MUT}$ was unable to block the expression of either GFP or Gluc (Fig. 4A and B). These results could be explained by differences in the efficiency of the frameshift between $PA_{WT}$, $PA_{PMUT}$, and $PA_{MUT}$ (16, 35). According to these results, when PA protein expression levels were evaluated by Western blotting, $PA_{WT}$ and $PA_{PMUT}$, which efficiently blocked GFP and Gluc expression, showed slightly lower PA protein levels than $PA_{MUT}$ (Fig. 4C). We were

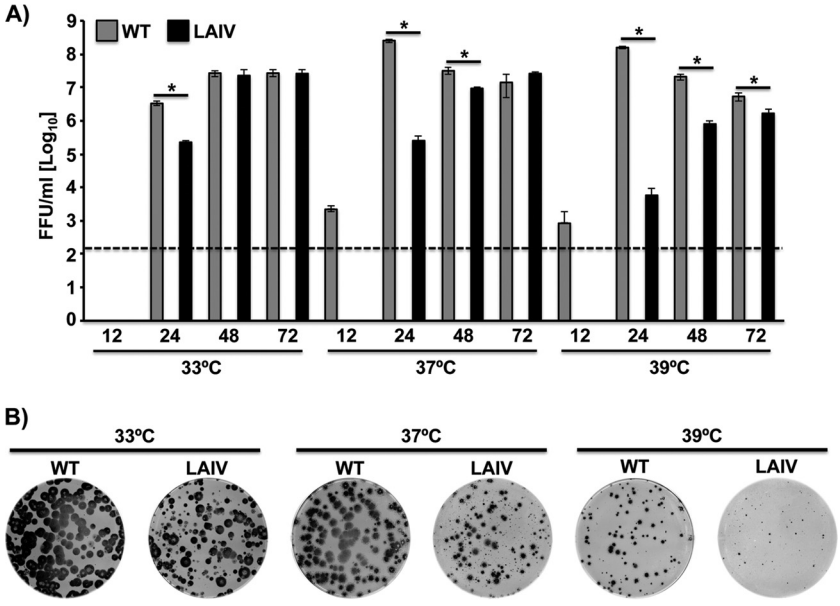


**FIG 2** Characterization of the pH1N1 LAIV virus. (A) Viral growth kinetics. TCS of MDCK cells infected at a low MOI (0.001) with pH1N1 WT (gray bars) or LAIV (black bars) virus at 33°C, 37°C, and 39°C were analyzed at the indicated times p.i. (12, 24, 48, and 72 h) by immunofocus assay using an anti-NP MAb (HB-65). Data represent the means and SDs of the results determined from triplicate wells. The dashed line indicates the limit of detection (200 FFU/ml). *, $P < 0.05$ (WT versus LAIV) using Student's *t* test ($n = 3$ per time point) from Microsoft Excel. (B) Plaque assays. MDCK cells were infected with pH1N1 WT and LAIV viruses and incubated at 33°C, 37°C, and 39°C for 3 days. The plaques phenotype was assessed by immunostaining with an anti-NP MAb (HB-65).

not able to detect PA-X expression by Western blotting, most likely due to the low frameshift efficiency (around 1.3%) (15). However, taking into account that the PA-X protein has a much stronger endonucleolytic activity than the PA protein (15, 18) and that the amino acid sequence of the PA protein is the same in all the constructs, is very likely that the mutations introduced in the frameshift of the $PA_{MUT}$ construct, but not those introduced in the $PA_{PMUT}$ construct, decreased PA-X protein expression levels, leading to a lower inhibition of general gene expression mediated by the PA-X protein.

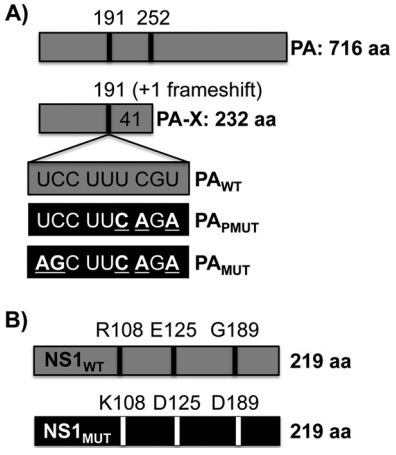


**FIG 3** Schematic representation of WT and mutant PA and NS1 proteins. (A) PA (top) and PA-X (bottom) WT viral proteins (gray) and the different mutations (black) introduced into the frameshift motif ($PA_{PMUT}$ or $PA_{MUT}$) to abolish PA-X expression are shown. Numbers on the right indicate the lengths of the PA and PA-X proteins. (B) NS1 WT (gray) and mutant (black) proteins containing amino acid substitutions allowing binding to CPSF30 and inhibition of host protein expression ($NS1_{MUT}$). Numbers on the right signify the lengths of the WT and mutant NS1 proteins.

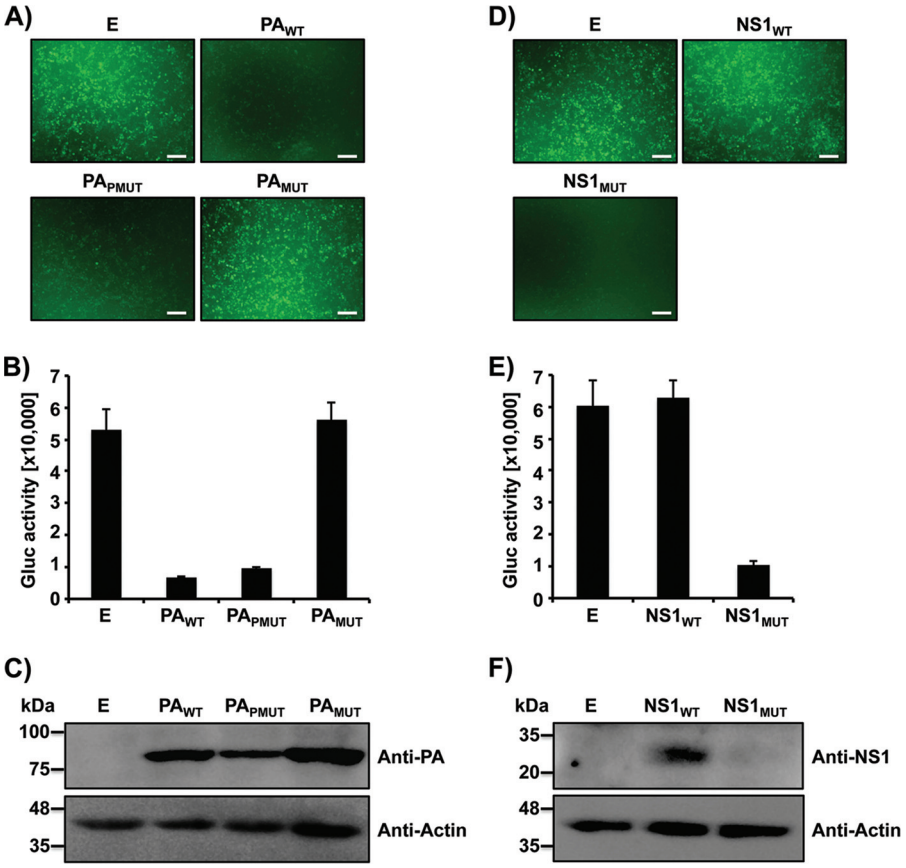


**FIG 4** Ability of WT and mutant PA-X and NS1 proteins to block host protein expression. Human 293T cells were transiently cotransfected, using LPF2000, with expression plasmids encoding GFP and Gluc under the control of a polymerase II promoter (pCAGGS GFP and pCAGGS Gluc, respectively) together with pDZ plasmids encoding WT or mutant (MUT) PA or NS1 proteins or empty (E) plasmid as a control. (A, B, D, and E) At 24 h p.t., cells were analyzed by GFP expression under a fluorescence microscope (A and D) and by Gluc activity from TCS (B and E). Representative images are shown. Scale bar = 100 $\mu$m. Results represent the means and standard deviations of triplicate values. (C and F) Protein expression from cell lysates was evaluated by Western blotting using specific antibodies for the viral PA and NS1 proteins or actin as loading control. Molecular markers are indicated on the left.

One of the mechanisms used by the IAV NS1 protein to counteract innate immune responses is the binding to CPSF30, which leads to host gene expression suppression, including expression of IFN and ISGs with antiviral activities (28, 30). It has been shown that the pH1N1 NS1 protein is unable to block host gene expression (34). However, amino acid changes R108K, E125D, and G189D (Fig. 3B) restored the ability of pH1N1 NS1 to bind to CPSF30 and to block host gene expression (34). Therefore, we introduced these amino acid changes into the NS1 of pH1N1 ($NS1_{MUT}$) (Fig. 3B). To demonstrate that these amino acid changes in pH1N1 NS1 lead to efficient blocking of host gene expression, 293T cells were cotransfected with pCAGGS plasmids expressing GFP and Gluc and with pDZ plasmids encoding $NS1_{WT}$ or $NS1_{MUT}$, or with the empty plasmid as an internal control (Fig. 4D to F). As previously shown (34), expression of the $NS1_{MUT}$ protein inhibited expression of GFP (Fig. 4D) and Gluc (Fig. 4E), whereas the $NS1_{WT}$ protein did not have an effect on reporter gene expression. These results were further confirmed when NS1 expression levels were analyzed by Western blotting (Fig. 4F). As expected, the $NS1_{MUT}$ protein, which efficiently blocked host gene expression, was not detected by Western blotting, whereas $NS1_{WT}$ expression was detected (Fig. 4F). These data confirmed that mutations R108K, E125D, and G189D restored the ability of the pH1N1 NS1 protein to inhibit host gene expression (34).

Next, we evaluated the interplay between PA-X and NS1 to block host gene expression in 293T cells transfected with both viral proteins (Fig. 5). To that end,

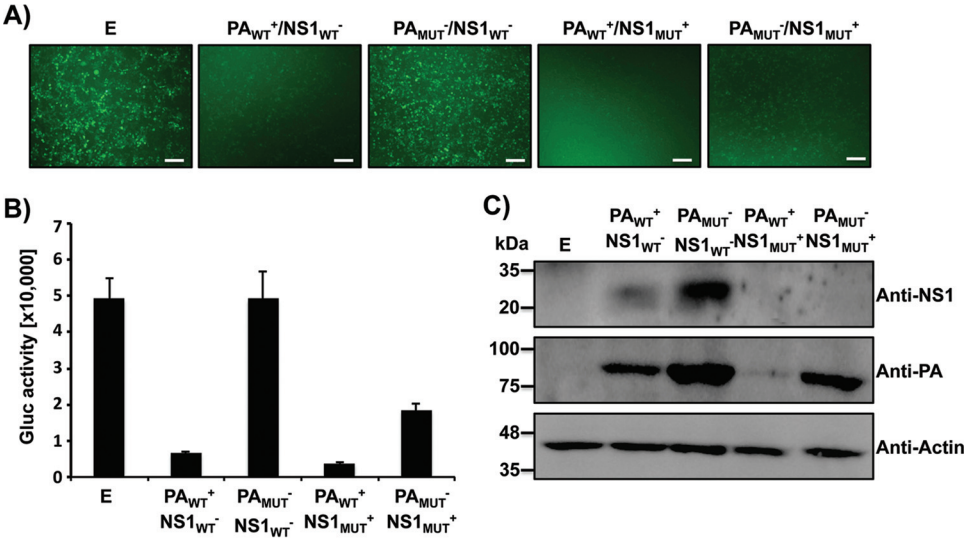


**FIG 5** Ability of PA-X and NS1 proteins to block host protein expression in combination. Human 293T cells were transiently cotransfected, using LPF2000, with pCAGGS GFP and pCAGGS Gluc together with the indicated combination of pDZ plasmids encoding WT or mutant (MUT) PA or NS1 proteins or empty (E) plasmid as a control. (A and B) At 24 h p.t., cells were analyzed for GFP expression under a fluorescence microscope (A) and for Gluc activity from TCS (B). Representative images are shown. Scale bar = 100 $\mu$m. Results represent the means and standard deviations of triplicate values. (C) Protein expression from cell lysates was evaluated by Western blotting using specific antibodies for the viral PA and NS1 proteins. Actin was used as a loading control. Molecular markers are noted on the left.

combinations of plasmids encoding $PA_{WT}^{+}$ or $PA_{MUT}^{-}$ and $NS1_{WT}^{-}$ or $NS1_{MUT}^{+}$ were cotransfected, and expression of GFP (Fig. 5A) and Gluc (Fig. 5B) was determined. Combinations containing $PA_{WT}^{+}$ or $NS1_{MUT}^{+}$ ($PA_{WT}^{+}/NS1_{WT}^{-}$, $PA_{WT}^{+}/NS1_{MUT}^{+}$, and $PA_{MUT}^{-}/NS1_{MUT}^{+}$) were able to inhibit the expression of both reporter genes (Fig. 5A and B). On the other hand, when $PA_{MUT}^{-}/NS1_{WT}^{-}$ were cotransfected together, an inhibition on the expression of either GFP or Gluc was not observed (Fig. 5A and B). Moreover, similar results were obtained when PA and NS1 protein expression levels were evaluated by Western blotting (Fig. 5C), confirming that $PA_{WT}^{+}$ and $NS1_{MUT}^{+}$ in combination were able to inhibit host gene expression.

**Effect of PA-X and NS1 on the activity of the viral polymerase.** To assess whether changes in PA-X expression due to mutations in the frameshift (Fig. 3A) could influence viral polymerase activity in the context of the generated pH1N1 LAIV viruses, a reporter MG assay was performed (Fig. 6A). pDZ plasmids encoding $PB2_{LAIV}$, $PB1_{LAIV}$, $PA_{WT}$, or $PA_{MUT}$ and NP were cotransfected in 293T cells, and Gluc expression was determined at 24 h p.t. We did not observed differences in Gluc expression in the MG assay, indicating that the activity of the polymerase complex containing either $PA_{WT}$ or $PA_{MUT}$ was similar in both cases. Next, to determine whether the NS1 protein could affect the polymerase activity, the MG assay was performed in the presence of $PA_{WT}$ or $PA_{MUT}$ together with $NS1_{WT}$ or $NS1_{MUT}$ (Fig. 6A). Under these conditions, a slight but significant reduction in the activity of the viral polymerase was observed when $PA_{MUT}$ was present in the polymerase complex ($PA_{MUT}^{-}/NS1_{WT}^{-}$ and $PA_{MUT}^{-}/NS1_{MUT}^{+}$). Moreover, protein expression levels for the components of the viral polymerase complex (PB2, PB1, and PA), NP, and NS1 were evaluated by Western blotting (Fig. 6B). Altogether, these findings suggest that the PA-X protein interplay with the NS1 protein can slightly affect the viral polymerase activity, at least in the context of the pH1N1 LAIV virus backbone. However, the mechanism involving the reduction in the activity of the viral polymerase complex is not totally understood and could involve the interaction of the viral proteins with cellular host factors (18, 44, 45).

**Generation and characterization of recombinant pH1N1 LAIV viruses with different abilities to inhibit host gene expression.** We next wanted to ascertain whether recombinant pH1N1 LAIV viruses encoding combinations of PA-X and NS1

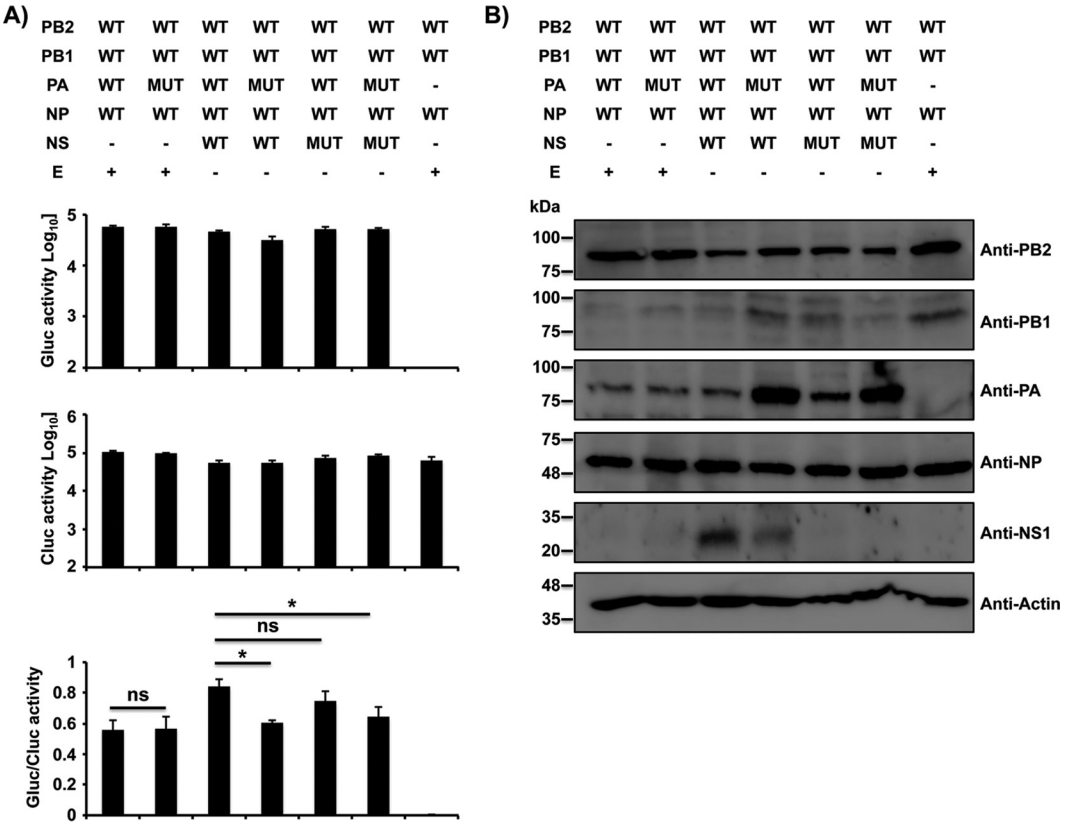


**FIG 6** (A) Effects of WT and mutant PA alone or in combination with NS1 on polymerase viral replication and transcription. Human 293T cells were transiently cotransfected, using LPF2000, with the pH1N1 LAIV ambisense pDZ expression plasmids encoding the minimal requirements for viral genome replication and gene transcription (PB2, PB1, and PA) and NP, together with the vRNA-like expression plasmid hpPol-I Gluc and the SV40-Cluc plasmid to normalize transfection efficiencies. Viral replication and transcription were evaluated at 24 h by Gluc expression. Gluc activity was normalized to that of Cluc. Data for Gluc (top), Cluc (middle), and Gluc activity normalized to that of Cluc (bottom) are shown. Data represent the means and SDs of the results determined from triplicate wells. *, $P < 0.05$ using Student's *t* test from Microsoft Excel. (B) Analysis of protein expression by Western blotting. Protein expression levels from cell lysates were evaluated by Western blotting using specific antibodies for the viral PB2, PB1, PA, NP, and NS1 proteins. Actin was used as a loading control. Molecular markers are noted on the left.

proteins with different abilities to block host gene expression or not could be rescued, as well as to assess the effect of the interplay between these two proteins in viral replication and pathogenesis. Therefore, we generated three more recombinant pH1N1 LAIV viruses containing $PA_{MUT}^{-}/NS1_{WT}^{-}$, $PA_{WT}^{+}/NS1_{MUT}^{+}$, or $PA_{MUT}^{-}/NS1_{MUT}^{+}$ (Fig. 7 and Table 1). We did not generated recombinant viruses containing only $PA_{MUT}$, based on the results shown in Fig. 4A to C. To analyze the replication properties of the recombinant pH1N1 LAIV viruses, we performed multicycle growth curves in MDCK (MOI, 0.001) or human A549 (MOI, 0.1) cells at 33°C (Fig. 7A and B, respectively). In MDCK cells, all viruses grew with similar titers, although the $PA_{MUT}^{-}/NS1_{WT}^{-}$ (which lacks the ability to inhibit host gene expression mediated by both viral proteins [Table 1]) and $PA_{WT}^{+}/NS1_{MUT}^{+}$ (expressing both viral proteins being able to counteract host gene expression [Table 1]) viruses replicated at slightly lower titers than the $PA_{WT}^{+}/NS1_{WT}^{-}$ and $PA_{MUT}^{-}/NS1_{MUT}^{+}$ viruses (Fig. 7A). The phenotypes of the recombinant pH1N1 LAIV viruses were further confirmed by plaque assay (Fig. 7C). Correlating with the multicycle growth kinetics in MDCK cells, the plaques of the $PA_{MUT}^{-}/NS1_{WT}^{-}$ and, more noticeably, $PA_{WT}^{+}/NS1_{MUT}^{+}$ viruses were smaller than those of the $PA_{WT}^{+}/NS1_{WT}^{-}$ or $PA_{MUT}^{-}/NS1_{MUT}^{+}$ viruses, where the ability to inhibit host gene expression was exchanged (Table 1). To evaluate if the pH1N1 LAIV viruses generated showed different replication kinetics in a cell line that more accurately represents the cells targeted in a natural human infection, we used A549 human lung epithelial cells (46,

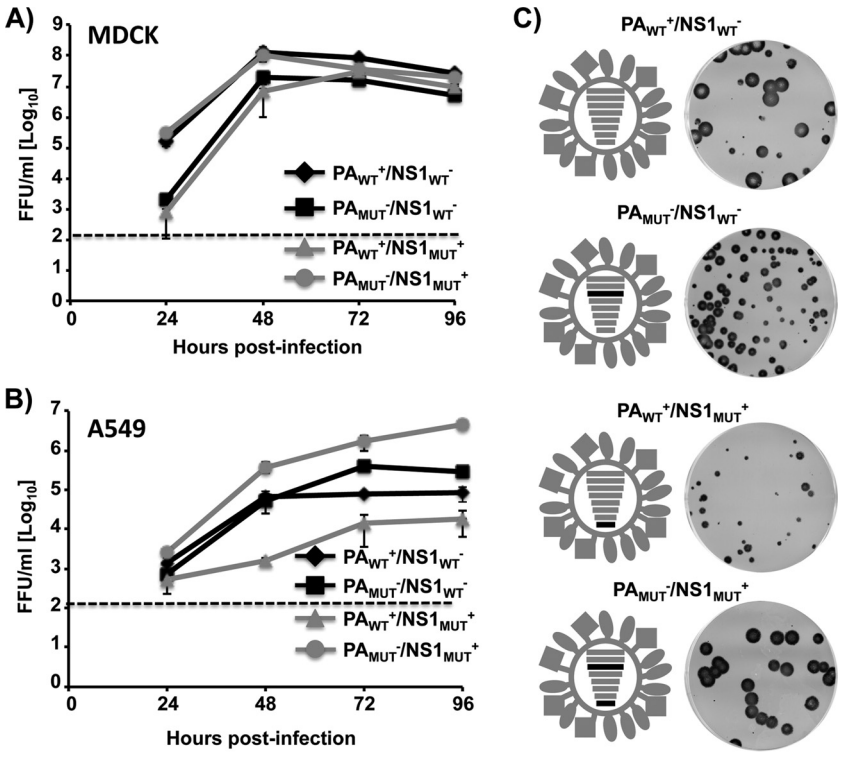


**FIG 7** Multicycle growth kinetics and plaque assay of pH1N1 LAIV viruses. (A and B) Viral growth kinetics. Canine MDCK (A) or human A549 (B) cells were infected (MOI of 0.001 for MDCK cells or 0.1 for A549 cells) with the indicated pH1N1 LAIV viruses and incubated at 33°C. TCS were collected at multiple times p.i., and viral titers were determined by immunofocus assay using an anti-NP MAb (HB-65). Data represent the means and SDs of the results determined from triplicate wells. The dashed line indicates the limit of detection (200 FFU/ml). (C) Plaque assays. MDCK cells were infected with the indicated pH1N1 LAIV viruses and incubated at 33°C for 3 days. Plaque phenotypes were assessed by immunostaining with the anti-NP monoclonal antibody HB-65. $PA_{WT}^{+}/NS1_{WT}^{-}$, virus containing WT PA and NS1 proteins. $PA_{MUT}^{-}/NS1_{WT}^{-}$, virus containing a mutant PA ($PA_{MUT}$) affecting its ability to inhibit host protein expression and a WT NS1. $PA_{WT}^{+}/NS1_{MUT}^{+}$, virus containing a WT PA and a mutant NS1 allowing inhibition of host protein expression. $PA_{MUT}^{-}/NS1_{MUT}^{+}$, virus containing both PA and NS1 mutants. In the virus illustrations, WT and mutant segments are indicated with gray and black lines, respectively.

47) (Fig. 7B). Interestingly, $PA_{MUT}^{-}/NS1_{MUT}^{+}$ virus, where NS1 but not PA-X is able to block host gene expression (Table 1), reached the highest titers. The $PA_{WT}^{+}/NS1_{WT}^{-}$ and $PA_{MUT}^{-}/NS1_{WT}^{-}$ viruses grew at slightly lower titers (5- to10-fold lower) than the $PA_{MUT}^{-}/NS1_{MUT}^{+}$ virus. On the other hand, and similar to the situation in MDCK cells (Fig. 7A), we observed a 100-fold decrease in viral titers for the $PA_{WT}^{+}/NS1_{MUT}^{+}$ virus, in which both PA-X and NS1 are able to inhibit the protein expression (Table 1). Altogether, these data suggest that the cooperation between the PA-X and NS1 proteins to block host gene expression can affect virus fitness in cells targeted during natural human infection.

**TABLE 1** Properties of pH1N1 LAIV viruses

| Property | $PA_{WT}^{+}$ $NS_{WT}^{-}$ virus | $PA_{MUT}^{-}$ $NS_{WT}^{-}$ virus | $PA_{WT}^{+}$ $NS1_{MUT}^{+}$ virus | $PA_{MUT}^{-}$ $NS1_{MUT}^{+}$ virus |
|---|---|---|---|---|
| Inhibition of host gene expression[a] | + − | − − | + + | − + |
| Viral replication *in vitro* | High | Low | Low | High |
| $MLD_{50}$ (PFU/mouse)[b] | 681 | 68,129 | $>10^5$ | 2,371 |
| Viral replication in mouse lungs | High | Low | Low | High |
| Induction of innate immune response in mice | + | − | − | + |
| Induction of adaptive immune response in mice | + | − | − | + |

[a]PA (left) and NS1 (right) proteins with (+) or without (−) the ability to inhibit host gene expression.
[b]Mortality was determined over 2 weeks ($n = 5$).

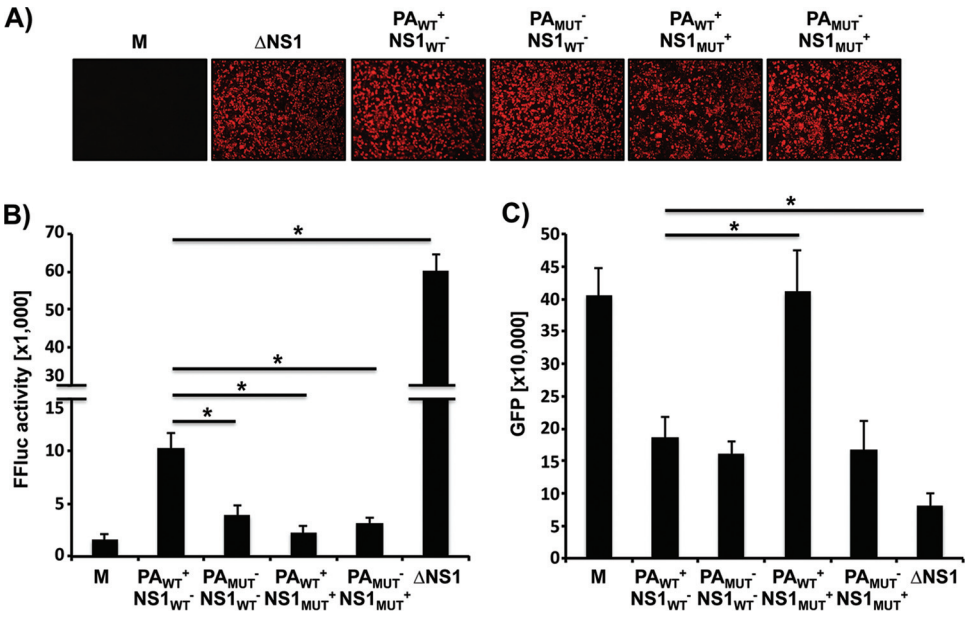


**FIG 8** Induction of IFN by pH1N1 LAIV viruses. MDCK cells constitutively expressing GFP-CAT and Fluc reporter genes under the control of the IFN-$\beta$ promoter (MDCK IFN-$\beta$-GFP/IFN-$\beta$-Fluc) were infected (MOI, 3) with the different pH1N1 LAIV viruses. Cells infected with an NS1 deficient PR8 virus (ΔNS1) were used as internal control. (A) Viral infections were evaluated by immunofluorescence using an anti NP MAb (HB-65). (B) At 16 h p.i., IFN-$\beta$ promoter activation was determined by Fluc expression. (C) Supernatants from infected MDCK IFN-$\beta$ GFP-CAT/Fluc cells were collected at the same time p.i. and, after UV virus inactivation, used to treat fresh MDCK cells for 24 h prior to infection with rNDV-GFP. GFP expression from infected cells was determined at 24 h p.i. using a microplate reader. *, $P < 0.05$ using Student's $t$ test from Microsoft Excel.

**Induction of IFN by recombinant pH1N1 LAIV viruses.** One of the main functions of the IAV NS1 and PA-X proteins is to counteract the IFN and host inflammatory responses during viral infection (12–14, 24, 27). Thus, to investigate the impact of the interplay between PA-X and NS1 to escape the antiviral response induced by cells after viral infection, we used two complementary cell-based and virus-based bioassays (Fig. 8). The cell-based assay involves MDCK cells constitutively expressing GFP and the firefly luciferase (Fluc) reporter gene under the control of the IFN-$\beta$ promoter (MDCK IFN-$\beta$-GFP/IFN-$\beta$-Fluc) (48). Cells were mock infected or infected (MOI, 3) with the pH1N1 LAIV viruses or a PR8 NS1-deficient (ΔNS1) virus, a good inducer of IFN responses (13), and IFN-$\beta$ promoter activation was evaluated. Importantly, comparable levels of viral infection were confirmed by immunofluorescence (Fig. 8A). As expected, Fluc expression was higher in cells infected with the ΔNS1 virus (Fig. 8B). However, although Fluc induction was inhibited upon infection with all the pH1N1 LAIV viruses, we observed slight differences in the activation of the IFN-$\beta$ promoter. IFN-$\beta$ promoter activation was slightly lower (about 2-fold) in cells infected with the PA$_{MUT}^{-}$/NS1$_{WT}^{-}$, PA$_{WT}^{+}$/NS1$_{MUT}^{+}$, or PA$_{MUT}^{-}$/NS1$_{MUT}^{+}$ virus than in PA$_{WT}^{+}$/NS1$_{WT}^{-}$ virus-infected cells, suggesting that all viruses were able to counteract IFN-$\beta$ induction. Next, we evaluated the presence of IFN in TCS from the same virus-infected MDCK cells using a virus-based assay, where inhibition of infection with recombinant Newcastle disease virus expressing GFP (rNDV-GFP) was evaluated (49). In this assay, the level of IFN in TCS from virus-infected cells results in inhibition of NDV infection and therefore GFP expression (50, 51). In cells pretreated with UV-inactivated TCS from mock- and PA$_{WT}^{+}$/NS1$_{MUT}^{+}$-infected cells, rNDV-GFP replicated efficiently (Fig. 8C), as expected based on the levels of IFN-$\beta$ promoter activation (Fig. 8B). However, levels of rNDV-GFP infection decreased in MDCK cells pretreated with TCS from PA$_{WT}^{+}$/NS1$_{WT}^{-}$, PA$_{MUT}^{-}$/NS1$_{WT}^{-}$, or PA$_{MUT}^{-}$/NS1$_{MUT}^{+}$ virus-infected cells (Fig. 8C). Inhibition of NDV was more evident, as expected, in cells pretreated with TCS from ΔNS1 virus-infected MDCK cells. Altogether, these data suggest that pH1N1 LAIV viruses inhibit the antiviral states induced in infected

cells to different extents. Viruses encoding PA-X and NS1 proteins that inhibit general gene expression ($PA_{WT}^{+}/NS1_{MUT}^{+}$) (Table 1) are the ones that best inhibit the IFN response, as expected.

**Virulence of pH1N1 LAIV viruses *in vivo*.** As the pH1N1 LAIV viruses showed differences in growth *in vitro* (Fig. 7), we also compared the virulence of pH1N1 LAIV viruses in mice (Fig. 9). To ascertain whether the ability of the PA-X and NS1 proteins to inhibit host gene expression could impact the course of an *in vivo* infection, groups of mice ($n = 5$) were inoculated with $10^2$, $10^3$, $10^4$, or $10^5$ PFU of the $PA_{WT}^{+}/NS1_{WT}^{-}$ (Fig. 9A), $PA_{MUT}^{-}/NS1_{WT}^{-}$ (Fig. 9B), $PA_{WT}^{+}/NS1_{MUT}^{+}$ (Fig. 9C), or $PA_{MUT}^{-}/NS1_{MUT}^{+}$ (Fig. 9D) virus and monitored for 14 days for body weight loss (left panels) and mortality (right panels). As expected, viruses containing the segment $PA_{MUT}$ or $NS1_{MUT}$ showed levels of attenuation and pathogenicity different from those for the $PA_{WT}^{+}/NS1_{WT}^{-}$ virus (Table 1), and the increased morbidity and mortality correlated with virus dose (Fig. 9). All mice infected with $10^4$ to $10^5$ PFU of the $PA_{WT}^{+}/NS1_{WT}^{-}$ virus rapidly lost weight, and none survived by day 8 or 10 p.i., respectively, while 40% of mice survived infection with $10^3$ PFU (Fig. 9A). In contrast, the $PA_{MUT}^{-}/NS1_{WT}^{-}$ and $PA_{WT}^{+}/NS1_{MUT}^{+}$ viruses showed high levels of attenuation (Fig. 9B and C, respectively). Only mice inoculated with $10^5$ PFU of the $PA_{MUT}^{-}/NS1_{WT}^{-}$ virus lost weight and succumbed (60%) to viral infection (Fig. 9B). Remarkably, none of the mice infected with the $PA_{WT}^{+}/NS1_{MUT}^{+}$ virus showed signs of weight loss or mortality (Fig. 9C). Interestingly, mice infected with the $PA_{MUT}^{-}/NS1_{MUT}^{+}$ virus (Fig. 9D) showed similar body weight loss and mortality as mice infected with the same doses of $PA_{WT}^{+}/NS1_{WT}^{-}$ virus (Fig. 9A). From these experiments, the 50% mouse lethal doses ($MLD_{50}$) (52) for the pH1N1 LAIV viruses were 681 PFU for $PA_{WT}^{+}/NS1_{WT}^{-}$ (Fig. 9A), 68,129 PFU for $PA_{MUT}^{-}/NS1_{WT}^{-}$ (Fig. 9B), greater than $10^5$ PFU for $PA_{WT}^{+}/NS1_{MUT}^{+}$ (Fig. 9C), and 2,371 PFU for $PA_{MUT}^{-}/NS1_{MUT}^{+}$ (Table 1).

To analyze whether the observed attenuation correlated with virus replication, we also evaluated viral titers in the lungs of infected mice (Fig. 10A and Table 1). To that end, groups of mice ($n = 3$) were inoculated with $10^3$ PFU of the different pH1N1 LAIV viruses, and viral titers were calculated at days 1, 3, and 5 p.i. Animals infected with the $PA_{WT}^{+}/NS1_{WT}^{-}$ or $PA_{MUT}^{-}/NS1_{MUT}^{+}$ virus showed similar viral titers at all days evaluated (Fig. 10A). Notably, virus replication in mouse lungs was limited after infection with the $PA_{MUT}^{-}/NS1_{WT}^{-}$ or $PA_{WT}^{+}/NS1_{MUT}^{+}$ virus (Fig. 10A), correlating with the very low morbidity and mortality observed (Fig. 9). We were not able to detect $PA_{WT}^{+}/NS1_{MUT}^{+}$ infectious particles at any day p.i., and we were able to detect $PA_{MUT}^{-}/NS1_{WT}^{-}$ infectious particles only at day 5 p.i. (Fig. 10A). We also measured mRNA expression levels of the viral M1 in the lungs of infected mice (Fig. 10B). While all the viruses were able to replicate in the lungs, correlating with the viral titers (Fig. 10A), the $PA_{WT}^{+}/NS1_{WT}^{-}$ and $PA_{MUT}^{-}/NS1_{MUT}^{+}$ viruses showed higher viral M1 mRNA expression levels than the $PA_{MUT}^{-}/NS1_{WT}^{-}$ and $PA_{WT}^{+}/NS1_{MUT}^{+}$ viruses (Fig. 10B). Overall, these data suggest that pH1N1 LAIV viruses that simultaneously encode PA-X and NS1 proteins that contain ($PA_{WT}^{+}/NS1_{MUT}^{+}$) or do not contain ($PA_{MUT}^{-}/NS1_{WT}^{-}$) the ability to block host gene expression are highly attenuated *in vitro* and *in vivo* (Table 1). On the other hand, the ability to inhibit host gene expression can be exchanged between PA-X and NS1 ($PA_{WT}^{+}/NS1_{WT}^{-}$ and $PA_{MUT}^{-}/NS1_{MUT}^{+}$) without significantly affecting pathogenesis and viral replication *in vitro* and *in vivo* (Table 1).

**Induction of innate and humoral immune responses.** The host response to virus infection has an important role in viral pathogenicity, and an exacerbated inflammatory response after IAV infection can be adverse to host survival (53, 54). To determine the impact of different expressions of PA-X in combination with the $NS1_{WT}$ or $NS1_{MUT}$ protein on the host antiviral immune response, we assessed the expression of cytokine genes in the lungs of infected mice (Fig. 11). Groups of mice ($n = 3$) inoculated with $10^3$ PFU of the different pH1N1 LAIV viruses were sacrificed at 1, 3, and 5 days p.i., and the induction of IFN-$\beta$ (Fig. 11A), tumor necrosis factor alpha (TNF-$\alpha$) (Fig. 11B), and chemokine (C-C motif) ligand 2 (CCL2) (Fig. 11C) mRNAs in the lungs was evaluated by

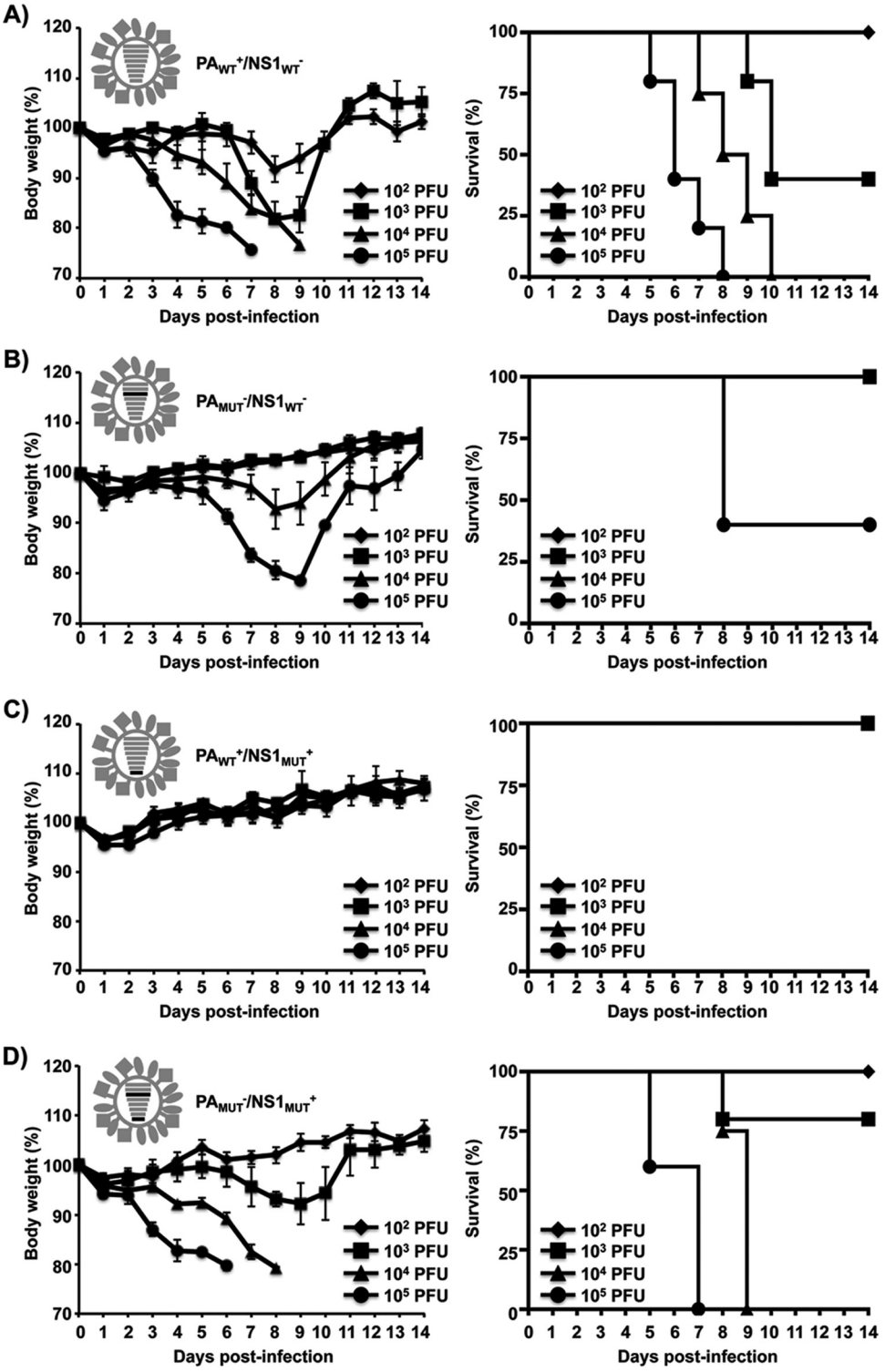


**FIG 9** Virulence of pH1N1 LAIV viruses. Six- to 8-week-old female C57BL/6 mice ($n = 5$) were infected i.n. with the indicated PFU of pH1N1 LAIV PA$_{WT}^{+}$/NS1$_{WT}^{-}$ (A), PA$_{MUT}^{-}$/NS1$_{WT}^{-}$ (B), PA$_{WT}^{+}$/NS1$_{MUT}^{+}$ (C), and PA$_{MUT}^{-}$/NS1$_{MUT}^{+}$ (D) viruses and then monitored daily for 2 weeks for body weight loss (left) and survival (right). Mice that lost 25% of their initial body weight were sacrificed. Data represent the means and SDs of the results determined for individual mice ($n = 5$).

reverse transcription-quantitative PCR (RT-qPCR). The PA$_{WT}^{+}$/NS1$_{WT}^{-}$ and PA$_{MUT}^{-}$/NS1$_{MUT}^{+}$ viruses, where the ability to block the gene expression was switched between the PA-X and the NS1 proteins (Table 1), induced strong cytokine responses *in vivo* at days 3 and 5 p.i. On the other hand, the PA$_{MUT}^{-}$/NS1$_{WT}^{-}$ and PA$_{WT}^{+}$/NS1$_{MUT}^{+}$ viruses

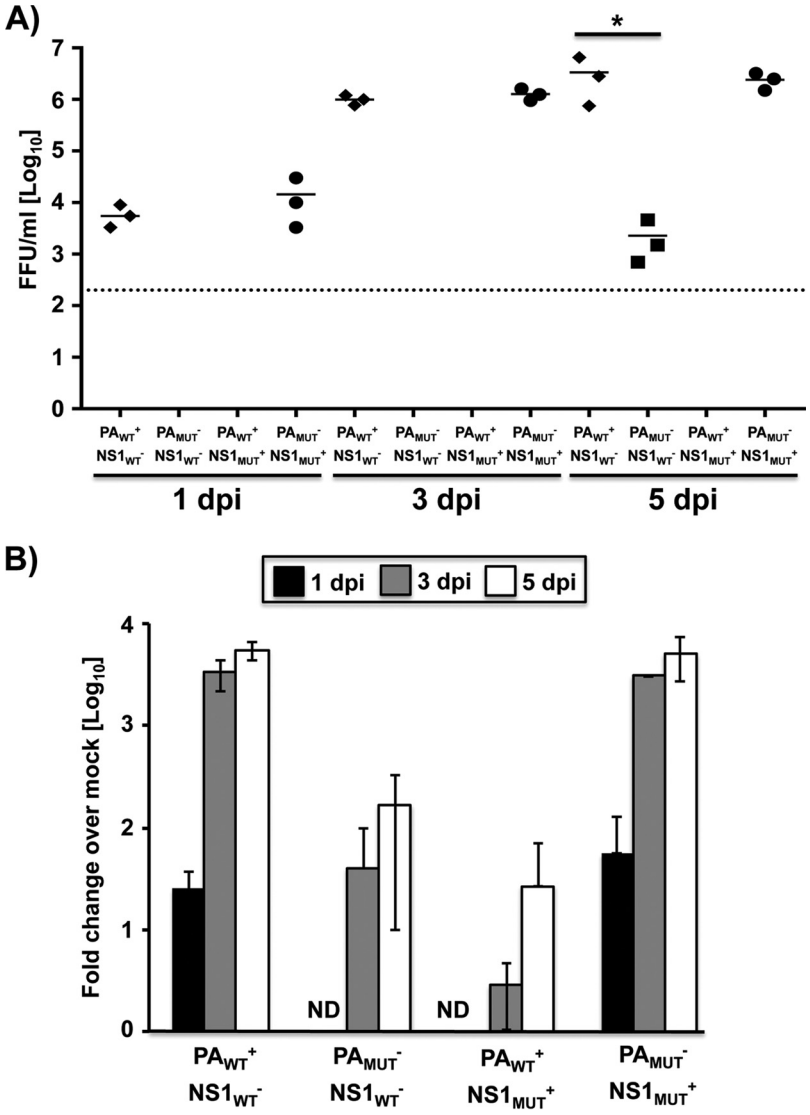


**FIG 10** Replication of pH1N1 LAIV viruses in mouse lungs. Six- to eight-week-old female C57BL/6 mice ($n = 9$) were infected i.n. with $1 \times 10^3$ PFU of the indicated pH1N1 LAIV viruses. (A) Viral replication in the lungs of infected mice was evaluated at 1, 3, and 5 days p.i. (dpi) ($n = 3$) by immunofocus assay using an anti-NP MAb (HB-65). Symbols represent data from individual mice. Bars represent the geometric means of lung viral titers. The dotted line represents the limit of detection of the assay (200 FFU/ml). *, $P < 0.05$ using Student's $t$ test ($n = 3$ per time point) from Microsoft Excel. (B) mRNA expression levels of the viral M1 in lungs of infected mice were quantified by RT-qPCR analysis. Fold expression changes in each mouse group were calculated relative to the control group of mock (PBS)-infected mice. Data represent the averages and SD values for three mice in each group on the days indicated.

barely induced detectable levels of IFN-$\beta$ or inflammatory immune responses at any day p.i. This is most likely due to the $PA_{WT}{}^{+}/NS1_{WT}{}^{-}$ and $PA_{MUT}{}^{-}/NS1_{MUT}{}^{+}$ pH1N1 LAIV viruses actively replicating in the lungs to induce significant inflammatory responses, whereas replication of the $PA_{MUT}{}^{-}/NS1_{WT}{}^{-}$ and, more notably, $PA_{WT}{}^{+}/NS1_{MUT}{}^{+}$ pH1N1 LAIV viruses is highly attenuated (Fig. 10).

In addition, we also evaluated humoral immune responses in sera collected 21 days after infection (dose of $10^2$ PFU) by enzyme-linked immunosorbent assay (ELISA) (Fig. 12 and Table 1), using cell extracts from pH1N1 virus-infected MDCK cells (Fig. 12A) or pH1N1 purified hemagglutinin (HA) (Fig. 12B) or NA (Fig. 12C) viral proteins. As expected, antibodies specific to total viral proteins, HA, and NA were detected at similar levels in sera from mice infected with the $PA_{WT}{}^{+}/NS1_{WT}{}^{-}$ and $PA_{MUT}{}^{-}/NS1_{MUT}{}^{+}$ viruses. However, and consistent with the data shown in Fig. 10 and 11, antibody levels

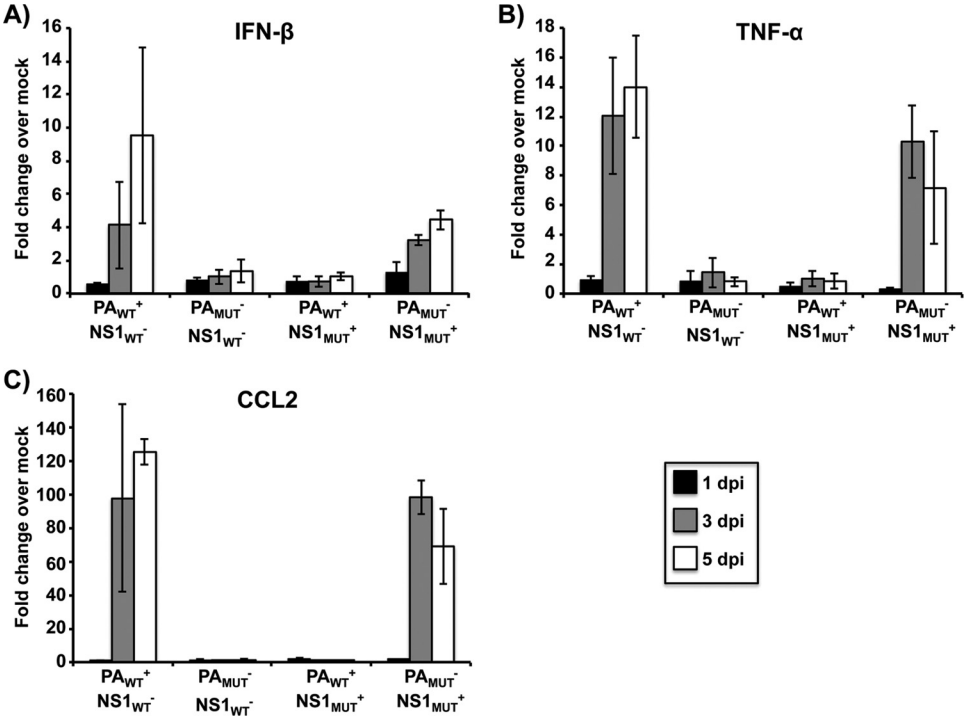


**FIG 11** Induction of innate immune responses by pH1N1 LAIV viruses. mRNA expression levels of IFN-$\beta$, TNF-$\alpha$ and CCL2 in lungs of mice infected with $1 \times 10^3$ PFU of the indicated pH1N1 LAIV viruses at 1, 3, and 5 dpi ($n = 3$) were quantified by RT-qPCR analysis. Fold expression changes in each mouse group were calculated relative to the control group of mock (PBS)-infected mice. Data represent the averages and SD values for three mice in each group on the days indicated.

were lower in serum samples from mice infected with the $PA_{MUT}^-/NS1_{WT}^-$ virus or undetectable in mice infected with the $PA_{WT}^+/NS1_{MUT}^+$ virus. Additionally, we performed hemagglutination inhibition (HAI) assays to examine the presence of neutralizing antibodies in the sera of immunized mice (Fig. 12D). Protective HAI titers against pH1N1 virus were observed only in animals infected with the $PA_{WT}^+/NS1_{WT}^-$ and $PA_{MUT}^-/NS1_{MUT}^+$ viruses. Altogether, these data suggest that the interplay of the PA-X and NS1 proteins to block host gene expression is important for viral replication and to regulate both innate and humoral host immune responses.

## DISCUSSION

Since the influenza virus PA-X and NS1 proteins were identified, multiple functions for these viral factors have been described (14, 15, 18, 29). Notably, the PA-X and NS1 from some IAV strains have the synergistic ability to block the host protein synthesis, although to do that, PA-X and NS1 use different mechanisms (14, 15, 17, 18, 29). It has been previously shown that the PA-X and NS1 proteins from pH1N1 can and cannot, respectively, suppress host protein expression, and a correlation between their individual function and viral replication and pathogenesis has also been described (34, 35, 43). Studies on the contribution of PA-X to viral pathogenicity showed IAV strain-specific differences (15, 20, 22, 35, 42, 43). Jagger et al. showed that PA-X expression reduced the viral pathogenicity of 1918 H1N1 IAV (15). Similarly, Gao et al. (43) and Hu et al. (16) reported that loss of PA-X expression increased viral replication and pathogenicity of pH1N1 and H5N1 IAVs. In contrast, recent work has described that loss of PA-X in pH1N1 or H9N2 viruses leads to a reduction in viral pathogenicity (21, 35). In addition, IAV strain-specific differences in the ability to block the cellular protein synthesis have also been reported (25, 31–33).

In contrast to preceding work, where the functions of these two proteins were studied individually, in this work we have investigated the interplay between PA-X and NS1 and the impact of their coordinated ability to block, or not, host gene expression

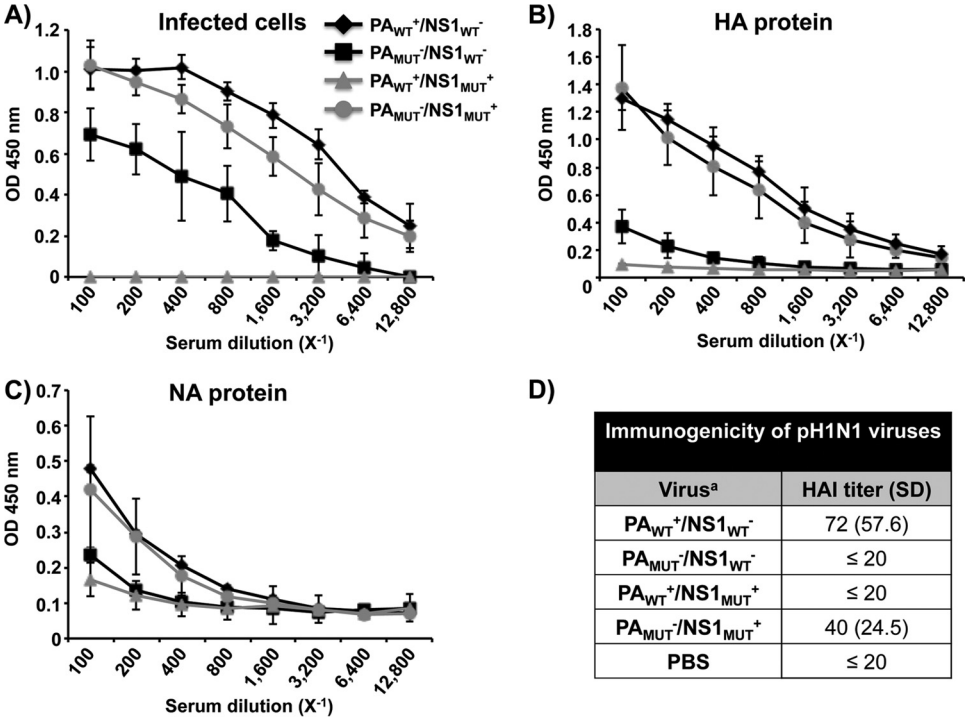


D)

| Immunogenicity of pH1N1 viruses | |
|---|---|
| Virus[a] | HAI titer (SD) |
| PA$_{WT}^{+}$/NS1$_{WT}^{-}$ | 72 (57.6) |
| PA$_{MUT}^{-}$/NS1$_{WT}^{-}$ | ≤ 20 |
| PA$_{WT}^{+}$/NS1$_{MUT}^{+}$ | ≤ 20 |
| PA$_{MUT}^{-}$/NS1$_{MUT}^{+}$ | 40 (24.5) |
| PBS | ≤ 20 |

**FIG 12** Humoral responses to pH1N1 LAIV viral infections. Six- to 8-week-old female C57BL/6 mice ($n = 5$) were infected i.n. with $1 \times 10^2$ PFU of the indicated pH1N1 LAIV viruses. (A to C) At 21 days p.i., mice were bled and sera were collected and evaluated by ELISA for IgG antibodies against total influenza virus proteins using cell extracts of pH1N1 virus-infected MDCK cells (A) or recombinant pH1N1 HA (B) or NA (C) protein. OD, optical density. (D) HAI titers from mock (PBS)-infected or infected mouse sera were calculated.

in the pathogenesis of IAV. To that end, we took advantage of a pH1N1 LAIV virus backbone (Fig. 1 and 2). The pH1N1 LAIV model allowed us to assess the contributions of PA-X and NS1 *in vitro* and *in vivo* while bypassing biosafety concerns and presenting a clearer phenotype. Moreover, pH1N1 WT is highly pathogenic in mice (55), and therefore it is difficult to measure subtle phenotypic differences, contrary to the situation with the pH1N1 LAIV variant that is less pathogenic *in vivo* (Fig. 9 and Table 1). Our results showed that simultaneous expression of both proteins that have the ability (PA$_{WT}^{+}$/NS1$_{MUT}^{+}$) (Table 1)or do not have the ability (PA$_{MUT}^{-}$/NS1$_{WT}^{-}$) (Table 1) to block host gene expression (Fig. 3 to 5) severely reduces viral replication *in vitro* (Fig. 7) and *in vivo* (Fig. 10) as well as pathogenicity in a mouse model of infection (Fig. 9 and Table 1). In contrast, when the ability to inhibit host protein synthesis switched between the PA-X and NS1 proteins, the new virus (PA$_{MUT}^{-}$/NS1$_{MUT}^{+}$) (Table 1) displayed viral replication *in vitro* and *in vivo* (Fig. 7 and 9, respectively) and virulence *in vivo* (Fig. 9 and Table 1) that were similar to those observed with a virus expressing both WT proteins (PA$_{WT}^{+}$/NS1$_{WT}^{-}$) (Table 1).

Our results show that a virus not expressing PA-X protein (PA$_{MUT}^{-}$/NS1$_{WT}^{-}$) (Fig. 7) and therefore lacking the ability to inhibit host gene expression by either PA-X or NS1 (Fig. 4 and 5 and Table 1) is attenuated compared to a virus expressing the WT PA-X and NS1 proteins (PA$_{WT}^{+}$/NS1$_{WT}^{-}$) (Fig. 9 and Table 1). These data are consistent with previous findings describing that a pH1N1 WT virus showed a slightly increased virulence in mice compared to a virus expressing lower levels of the PA-X protein (21, 35). Remarkably, by using our pH1N1 LAIV virus, we have observed greater differences in virus pathogenicity than those observed using pH1N1 WT, suggesting that the LAIV virus backbone is better suited to detect differences in pathogenicity than the WT backbone. On the other hand, contrary to other studies (35), we did not observe a higher innate (Fig. 11) or humoral (Fig. 12) response with the PA-X-deficient virus in mice. This is most likely due to the very reduced viral replication in mouse lungs

observed for the $PA_{MUT}^{-}/NS1_{WT}^{-}$ virus (Fig. 10), which could be explained, at least in part, by the lower levels of polymerase activity observed with the $PA_{MUT}$ protein than with $PA_{WT}$ in the presence of the NS1 protein (Fig. 6).

Furthermore, we evaluated the virulence of a virus harboring two proteins with the ability to inhibit the protein synthesis in the host ($PA_{WT}^{+}/NS1_{MUT}^{+}$) (Fig. 7 and Table 1). We observed that the virus replicated at lower levels in human A549 cells (Fig. 7), despite being able to efficiently control IFN-$\beta$ production induced after infection (Fig. 8). This phenotype could be a consequence of an excessive inhibition of host protein synthesis, which could be affecting the expression of multiple host factors required for efficient virus replication.

Accordingly, the $PA_{WT}^{+}/NS1_{MUT}^{+}$ virus was also highly attenuated *in vivo* (Fig. 9), inducing poor IFN and inflammatory (Fig. 11) or humoral (Fig. 12) responses, most likely because of its impaired replication in mouse lungs (Fig. 10). Previously, Hale et al. showed that a pH1N1 including three mutations in the NS1 protein (the same used in this work) that restored NS1's ability to block host gene expression induced less IFN-$\beta$ (as well as other cytokines) during infection (34). However, using an *in vivo* mouse model of infection, the virus was slightly less pathogenic, and it appeared to be cleared faster than the pH1N1 WT virus (34). Although those data correlate with our observations, using our pH1N1 LAIV model, this phenotype was more evident, reinforcing the idea that the LAIV virus backbone may represent a better approach to elucidating small differences in pathogenicity. Interestingly, a pH1N1 LAIV virus in which the ability to inhibit the host gene expression was interchanged between the PA-X and the NS1 proteins ($PA_{MUT}^{-}/NS1_{MUT}^{+}$) (Fig. 3 and Table 1) showed virulence (Fig. 9) and ability to replicate *in vitro* (Fig. 7) and *in vivo* (Fig. 10) similar to those of the pH1N1 LAIV WT virus (Table 1). Moreover, $PA_{MUT}^{-}/NS1_{MUT}^{+}$ pH1N1 LAIV virus was able to induce levels of IFN and cytokines (Fig. 11), as well as humoral responses (Fig. 12), similar to those for the pH1N1 LAIV WT virus, suggesting that inhibition of host gene expression is subject to a strict balance and that this function can be exchanged between the IAV PA-X and NS1 proteins.

Viruses need to hijack the cellular machinery for the progression of infection. Therefore, an exacerbated ($PA_{WT}^{+}/NS1_{MUT}^{+}$) blocking of host protein synthesis may compromise successful viral infection. Several cellular host factors have been described to be important for viral replication (56, 57). Thus, a strong inhibition of the expression of these cellular host factors could have a negative effect on viral replication. On the other hand, to replicate in the host, viruses have developed multiple mechanisms to counteract the innate immune response and the antiviral state produced in the infected cell and in the neighborhood cells. Thus, inhibition of host protein synthesis could contribute to dampening the antiviral response as well as to diverting the cellular resources toward viral replication. Taken together, our findings suggest that an optimal control of host gene expression mediated by PA-X and NS1 is required for the efficient viral replication in IFN-competent systems, showing that too much ($PA_{WT}^{+}/NS1_{MUT}^{+}$) or too little ($PA_{MUT}^{-}/NS1_{WT}^{-}$) inhibition of host protein expression can be deleterious for influenza viruses (Table 1).

Importantly, our findings suggest that the role of PA-X together with NS1 can be important to understand virus pathogenicity. In fact, the characterization of these two viral proteins could help to predict the virulence of new IAV strains with pandemic potential. Likewise, a balance of inhibition of host gene expression mediated by PA-X and/or NS1 would be required for efficient replication of LAIV viruses, without impairing their safety profile, to induce protective innate and humoral responses upon successful infection. However, more in-depth studies will be required in the future to fully understand the mechanism(s) underlying these changes in host gene expression mediated by the cooperative functions of the PA-X and NS1 proteins. Moreover, other IAV proteins (e.g., PB2 or PB1-F2) have been shown to play a role in inhibiting innate immune response (12, 27, 58) and should be further analyzed in the context of WT or mutant PA-X and NS1 proteins.

## MATERIALS AND METHODS

**Cells and viruses.** Human embryonic kidney (293T; ATCC CRL-11268), human lung epithelial carcinoma (A549; ATCC CCL-185), and Madin-Darby canine kidney (MDCK) (ATCC CCL-34) cells were grown in Dulbecco's modified Eagle's medium (DMEM) (Mediatech, Inc.) supplemented with 10% fetal bovine serum (FBS) (Atlanta Biologicals) and 1% penicillin (100 U/ml)–streptomycin (100 $\mu$g/ml)–2 mM L-glutamine (P-S-G) (Mediatech, Inc.) at 37°C in air enriched with 5% $CO_2$. MDCK cells constitutively expressing the green fluorescent protein (GFP) and firefly luciferase (Fluc) reporter genes under the control of the IFN-$\beta$ promoter (MDCK IFN-$\beta$-GFP/IFN-$\beta$-Fluc) were described previously (48).

Recombinant wild-type (WT) pandemic H1N1 influenza virus A/California/4_NYICE_E3/2009 (pH1N1) has been previously described (55). The recombinant pH1N1 LAIV virus was generated using plasmid-based reverse genetics techniques (39, 59). WT and LAIV pH1N1 viral titrations and stocks were produced at 33°C. Influenza virus A/Puerto Rico/8/34 H1N1 NS1-deficient (ΔNS1) virus (13) and the recombinant Newcastle disease virus expressing GFP (rNDV-GFP) were previously described (60).

**Plasmids.** To generate all the recombinant pH1N1 LAIV viruses, the PB2, PB1, PA, and NS viral segments were subcloned into a pUC19 plasmid (New England BioLabs). To generate $PB2_{LAIV}$ and $PB1_{LAIV}$, the *ts* mutations in PB2 (N265S) and PB1 (K391E, D581G, and A661T) were introduced by site-directed mutagenesis (7, 9, 10, 39). pH1N1 already contained the amino acid change D34G in the viral NP. PA-X-deficient plasmids were created by mutating the frameshift motif from UCC UUU CGU (WT) to UCC UUC AGA ($PA_{PMUT}$) or AGC UUC AGA ($PA_{MUT}$) (15, 16, 18–23, 35, 42, 43). Three amino acid substitutions (R108K, E125D, and G189D) were introduced into the NS segment to mutate the NS1 protein (34). Mutated PB2 ($PB2_{LAIV}$), PB1 ($PB1_{LAIV}$), PA ($PA_{PMUT}$ and $PA_{MUT}$), and NS1 ($NS1_{MUT}$) viral segments were subcloned from pUC19 into the ambisense pDZ plasmid for virus rescues (61). To test the polymerase activity using a minigenome (MG) assay, we engineered a pPolI plasmid containing the human RNA polymerase I (Pol-I) promoter and the mouse Pol-I terminator separated by SapI endonuclease restriction sites (hpPol-I). The *Gaussia* luciferase (Gluc) reporter gene ORF containing the 3′ and the 5′ noncoding regions of the NP viral RNA (vRNA) was cloned into the hpPol-I plasmid to generate the hpPol-I Gluc reporter plasmid. All plasmids were confirmed by sequencing (ACGT Inc.). Primers for the generation of the different plasmid constructs are available upon request.

**Rescue of recombinant pH1N1 LAIV viruses.** Virus rescues were performed as previously described (49, 62, 63). Cocultures (1:1) of 293T and MDCK cells in 6-well plates were cotransfected in suspension with 1 $\mu$g of each of the ambisense plasmids (pDZ-PB2 or $PB2_{LAIV}$, -PB1 or $PB1_{LAIV}$, -$PA_{WT}$ or $PA_{MUT}$, -HA, -NP, -NA, -M, and $NS_{WT}$ or $NS1_{MUT}$) using Lipofectamine 2000 (LPF2000) (Invitrogen). At 12 h posttransfection (p.t.), the transfection medium was replaced with DMEM containing 0.3% bovine serum albumin (BSA), 1% P-S-G, and 0.5 $\mu$g/ml of *N*-tosyl-L-phenylalanine chloromethyl ketone (TPCK)-treated trypsin (Sigma). At 72 h p.t., tissue culture supernatants (TCS) were collected, clarified, and used to infect fresh MDCK cells ($10^6$ cells/well, 6-well plate format). At 3 to 4 days postinfection (p.i.), recombinant viruses were plaque purified and scaled up in MDCK cells (49). Stocks were titrated by immunofocus assay (focus-forming units [FFU] per milliliter) on MDCK cells (49, 63). Virus stocks were confirmed by sequencing the PB2, PB1, PA, and NS1 ORFs using purified total RNA (TRIzol reagent; Invitrogen) from infected MDCK cells ($10^6$ cells/well, 6-well plate format) according to the manufacturer's specifications.

**Inhibition of host gene expression.** To evaluate the effect of pH1N1 NS1 and PA-X proteins on host protein synthesis, 293T cells ($2.5 \times 10^5$ cells/well, 24-well plate format, triplicates) were transiently cotransfected in suspension, using LPF2000, with 1 $\mu$g/well of the indicated pDZ plasmids encoding WT or mutant PA ($PA_{PMUT}$ and $PA_{MUT}$) proteins, NS1 WT and mutant ($NS1_{MUT}$) proteins, or empty (E) plasmid as control, together with 25 ng/well of pCAGGS plasmids expressing GFP (29) or Gluc (64). At 24 h p.t., cells were analyzed for GFP expression under a fluorescence microscope, and Gluc activity was quantified from TCS using a Biolux *Gaussia* luciferase reagent (New England BioLabs) and a Lumicount luminometer (Packard). The mean value and standard deviation (SD) were calculated using Microsoft Excel software.

**MG assays.** To evaluate the effect of WT and mutant NS1 and PA-X proteins on viral polymerase activity, 293T cells ($2.5 \times 10^5$ cells/well, 24-well plate format, triplicates) were transiently cotransfected in suspension, using LPF2000, with 125 ng of each ambisense pDZ plasmids encoding the $PB2_{LAIV}$, $PB1_{LAIV}$, PA ($PA_{WT}$ or $PA_{MUT}$), NP, and NS ($NS_{WT}$ or $NS1_{MUT}$) plasmids, together with 250 ng of the hpPol-I Gluc plasmid. A *Cypridina* luciferase-encoding plasmid (simian virus 30 [SV40]-Cluc, 50 ng) was also included to normalize transfection efficiencies (65, 66). Cells transfected in the absence of pDZ NP were used as a negative control. At 24 h p.t., Gluc and Cluc expression levels were determined using Biolux *Gaussia* or *Cypridina* luciferase assay kits (New England BioLabs) and a Lumicount luminometer (Packard). The mean value and standard deviation were calculated using Microsoft Excel software.

**Protein gel electrophoresis and Western blot analysis.** Proteins from transfected cell lysates were separated by denaturing electrophoresis using 10% SDS-polyacrylamide gels and transferred to a nitrocellulose membrane (Bio-Rad) with a Bio-Rad Mini Protean II electroblotting apparatus at 100 V for 2 h. Membranes were blocked for 1 h with 5% dried skim milk in phosphate-buffered saline (PBS) containing 0.1% Tween 20 (T-PBS) and incubated overnight at 4°C with primary rabbit or goat polyclonal antibodies (PAbs) against NS1 (67), PA (ABIN398948; Antibodies-Online), NP (67), PB2 (SC17603; Santa Cruz Biotechnology), or PB1 (SC117601; Santa Cruz Biotechnology) or a mouse monoclonal antibody (MAb) against NP (ATCC HB-65). Mouse MAb against actin (A1978; Sigma) was used as an internal loading control. Bound primary antibodies were detected with horseradish peroxidase (HRP)-conjugated antibodies against the different (mouse, rabbit, or goat) species (GE Healthcare). Proteins were detected by chemiluminescence (Thermo Fisher Scientific) following the manufacturer's recommendations and photographed using a Kodak ImageStation.

**Virus growth kinetics.** To determine virus growth kinetics *in vitro*, triplicate wells of confluent monolayers of MDCK or A549 cells ($4 \times 10^5$ cells/well, 12-well plate format) were infected at a multiplicity of infection (MOI) of 0.001 (MDCK) or 0.1 (A549). After 1 h of virus adsorption at room temperature, cells were overlaid with DMEM containing 0.3% BSA, antibiotics, and TPCK-treated trypsin (1 $\mu$g/ml for MDCK cells and 0.25 $\mu$g/ml for A549 cells) and incubated at 33°C, 37°C, or 39°C. At the indicated times p.i. (12, 24, 48, 72, and 96 h), TCS were collected and viral titers were determined by immunofocus assay (FFU/ml) as previously described (49, 63). Briefly, confluent wells of MDCK cells ($10^4$ cells/well, 96-well plate format, triplicates) were infected with 10-fold serial dilutions of TCS. At 12 h p.i., cells were fixed and permeabilized (4% formaldehyde and 0.5% Triton X-100 in PBS) for 15 min at room temperature. The cells were then incubated in blocking solution (2.5% BSA in PBS) for 1 h at room temperature and incubated with the influenza virus NP MAb HB-65 for 1 h at 37°C. After washing with PBS, cells were incubated with a fluorescein isothiocyanate (FITC)-conjugated rabbit anti-mouse IgG secondary antibody (Dako) for 1 h at 37°C. NP-expressing positive cells were enumerated to determine the virus titer (FFU/ml) (49, 63). The mean value and standard deviation (SD) were calculated using Microsoft Excel software.

**Plaque assay and immunostaining.** Confluent monolayers of MDCK cells ($10^6$ cells/well, 6-well plate format) were infected for 1 h at room temperature, and after virus adsorption, cells were overlaid with agar and incubated at 33°C, 37°C, or 39°C. At 3 days p.i., cells were fixed with 4% paraformaldehyde for 15 min at room temperature. After the overlays were removed, cells were permeabilized (0.5% Triton X-100 in PBS) for 15 min at room temperature and prepared for immunostaining as previously described (63, 68), using the NP MAb HB-65 and vector kits (Vectastain ABC kit and DAB HRP substrate kit: Vector) following the manufacturer's specifications.

**Bioassay to evaluate IFN production.** To evaluate the levels of IFN produced by infected cells, monolayers ($2.5 \times 10^5$ cells/well, 24-well plate format, triplicates) of MDCK cells constitutively expressing GFP and Fluc reporter genes under the control of the IFN-$\beta$ promoter (MDCK IFN-$\beta$-GFP/IFN-$\beta$-Fluc) (48) were mock infected or infected (MOI of 3) with the pH1N1 LAIV viruses. At 16 h p.i., activation of the IFN-$\beta$ promoter was determined by Fluc expression in cell lysates using a Promega luciferase reporter assay and a Lumicount luminometer. Influenza virus infection levels were evaluated by immunofluorescence using an anti-NP MAb (HB-65) as described above. In addition, TCS of infected MDCK cells were collected, and viruses were UV inactivated by exposure to short-wave (254-nm) UV radiation (Mineralight UV lamp, UV S-68; Ultra-Violet Products) for 40 min at a distance of 6 cm as previously described (25, 26, 49). Fresh MDCK cells seeded in 96-well plates ($10^4$ cells/well, triplicates) were then treated with the UV-inactivated TCS for 24 h and infected with rNDV-GFP (MOI, 3). The GFP intensity was measured, at 24 h p.i., with a microplate reader (DTX880; Beckman Coulter). GFP expression by mock-treated cells was considered to have a value of 100%. Mean values and standard deviations were calculated using Microsoft Excel software.

**Mouse experiments.** Female 6- to 8-week-old C57BL/6 mice were purchased from the National Cancer Institute (NCI) and maintained in the animal care facility at the University of Rochester under specific-pathogen-free conditions. All animal protocols were approved by the University of Rochester Committee of Animal Resources and complied with the recommendations in the *Guide for the Care and Use of Laboratory Animals* of the National Research Council (69). Mice were anesthetized intraperitoneally with 2,2,2-tribromoethanol (Avertin; 240 mg/kg of body weight) and then inoculated intranasally (i.n.) with 30 $\mu$l of the indicated pH1N1 LAIV virus. Mice were monitored daily for morbidity (body weight loss) and mortality (survival). Mice showing 25% loss of their initial body weight were considered to have reached the experimental endpoint and were humanely euthanized. The 50% mouse lethal doses ($MLD_{50}$) for the recombinant pH1N1 LAIV viruses was determined using the method of Reed and Muench (52). Virus replication was evaluated by determining viral titers in the lungs at 1, 3, and 5 days p.i. To that end, three mice in each group were sacrificed, and lungs were extracted and homogenized. Virus titers were determined by immunofocus assay (FFU/ml) as indicated above. Geometric mean titers (GMTs) were performed using GraphPad Prism software. Levels of IFN-$\beta$, TNF-$\alpha$, and CCL2 induction were analyzed in mouse lungs at 1, 3, and 5 days p.i. To that end, mice ($n = 3$) were sacrificed, and lungs were extracted and incubated in RNAlater (Ambion) at 4°C for 24 h prior to freezing at −80°C. Lungs were homogenized in lysis buffer using a gentleMACS dissociator (Miltenyi Biotec), and total RNA was extracted using an RNeasy minikit (Qiagen). Reverse transcriptase reactions were performed at 37°C for 2 h using the high-capacity cDNA transcription kit (Applied Biosystems) and an oligo(dT) primer to amplify mRNAs, starting from 300 ng of total RNA. Quantitative PCRs (qPCRs) were performed using a TaqMan gene expression assay (Applied Biosystems) specific for the viral M1 mRNA (NR-15592, Influenza Virus Real-Time RT-PCR Assay Influenza A & B viruses; Biodefense and Emerging Infectious Research Resources Repository [BEI Resources]), IFN-$\beta$ (Mm00439552_s1; Applied Biosystems), chemokine (C-C motif) ligand 2 (CCL2) (Mm00441242_m1; Applied Biosystems), and tumor necrosis factor alpha (TNF-$\alpha$) (Mm00443258_m1; Applied Biosystems) murine genes. Quantification was achieved using the $2^{-\Delta\Delta CT}$ method (70).

**ELISA.** Mouse sera were collected by submandibular bleeding at 21 days p.i. and evaluated for the presence of influenza virus-specific antibodies by enzyme-linked immunosorbent assay (ELISA) as previously described (49). Briefly, 96-well plates were coated for 16 h at 4°C with lysates from mock- or pH1N1 WT virus-infected MDCK cells. Alternatively, plates were coated with pH1N1 virus HA (200 ng per well) (FR-180 IRR) or NA (200 ng per well) (NR-19234; BEI Resources) recombinant protein. After washing with PBS, coated wells were blocked with PBS containing 1% BSA and then incubated with 1:2 dilutions (starting dilution of 1:100) of mouse serum at 37°C. After 1 h of incubation, plate wells were washed with $H_2O$ and incubated with HRP-conjugated goat anti-mouse IgG (GE Healthcare) for 30 min at 37°C. The reactions were developed with tetramethylbenzidine (TMB) substrate (BioLegend) for 10 min at room

temperature, quenched with 2 N $H_2SO_4$, and read at 450 nm (Vmax kinetic microplate reader; Molecular Devices).

**HAI assays.** Hemagglutination inhibition (HAI) assays were used to assess the presence of neutralizing antibodies (49). To that end, mouse sera were treated with receptor-destroying enzyme (RDE) (Denka Seiken) and heat inactivated for 30 min at 56°C. Sera were then serially 2-fold diluted (starting dilution of 1:20) in 96-well V-bottom plates and mixed 1:1 with 4 hemagglutinating units (HAU) of pH1N1 WT virus for 60 min at room temperature. The HAI titers were determined by adding 0.5% turkey red blood cells (RBCs) to the virus-antibody mixtures for 30 min on ice, as previously described (49).

## ACKNOWLEDGMENTS

The New York Influenza Center of Excellence (NYICE), a member of the NIAID Centers of Excellence for Influenza Research and Surveillance (CEIRS), partially supported this work (HHSN272201400005C).

We thank the Biodefense and Emerging Infectious Research Resources Repository (BEI Resources) and Influenza Research Resources (IRR) for providing reagents.

## REFERENCES

1. Palese P, Shaw ML. 2007. Orthomyxoviridae: the viruses and their replication. *In* Knipe DM, Howley PM, Griffin DE, Lamb RA, Martin MA (ed), Fields virology, 5th ed. Lippincott Williams and Wilkins, Philadelphia, PA.
2. Resa-Infante P, Jorba N, Coloma R, Ortin J. 2011. The influenza virus RNA synthesis machine: advances in its structure and function. RNA Biol 8:207–215. https://doi.org/10.4161/rna.8.2.14513.
3. Wong SS, Webby RJ. 2013. Traditional and new influenza vaccines. Clin Microbiol Rev 26:476–492. https://doi.org/10.1128/CMR.00097-12.
4. Chan W, Zhou H, Kemble G, Jin H. 2008. The cold adapted and temperature sensitive influenza A/Ann Arbor/6/60 virus, the master donor virus for live attenuated influenza vaccines, has multiple defects in replication at the restrictive temperature. Virology 380:304–311. https://doi.org/10.1016/j.virol.2008.07.027.
5. Cox NJ, Kitame F, Kendal AP, Maassab HF, Naeve C. 1988. Identification of sequence changes in the cold-adapted, live attenuated influenza vaccine strain, A/Ann Arbor/6/60 (H2N2). Virology 167:554–567.
6. Snyder MH, Betts RF, DeBorde D, Tierney EL, Clements ML, Herrington D, Sears SD, Dolin R, Maassab HF, Murphy BR. 1988. Four viral genes independently contribute to attenuation of live influenza A/Ann Arbor/6/60 (H2N2) cold-adapted reassortant virus vaccines. J Virol 62:488–495.
7. Cox A, Baker SF, Nogales A, Martinez-Sobrido L, Dewhurst S. 2015. Development of a mouse-adapted live attenuated influenza virus that permits in vivo analysis of enhancements to the safety of live attenuated influenza virus vaccine. J Virol 89:3421–3426. https://doi.org/10.1128/JVI.02636-14.
8. Jin H, Zhou H, Lu B, Kemble G. 2004. Imparting temperature sensitivity and attenuation in ferrets to A/Puerto Rico/8/34 influenza virus by transferring the genetic signature for temperature sensitivity from cold-adapted A/Ann Arbor/6/60. J Virol 78:995–998. https://doi.org/10.1128/JVI.78.2.995-998.2004.
9. Nogales A, Rodriguez L, Chauche C, Huang K, Reilly EC, Topham DJ, Murcia PR, Parrish CR, Martinez-Sobrido L. 31 January 2017. Temperature-sensitive live-attenuated canine influenza virus H3N8 vaccine. J Virol https://doi.org/10.1128/JVI.02211-16.
10. Rodriguez L, Nogales A, Reilly EC, Topham DJ, Murcia PR, Parrish CR, Martinez Sobrido L. 2017. A live-attenuated influenza vaccine for H3N2 canine influenza virus. Virology 504:96–106. https://doi.org/10.1016/j.virol.2017.01.020.
11. Zhou B, Li Y, Speer SD, Subba A, Lin X, Wentworth DE. 2012. Engineering temperature sensitive live attenuated influenza vaccines from emerging viruses. Vaccine 30:3691–3702. https://doi.org/10.1016/j.vaccine.2012.03.025.
12. Iwasaki A, Pillai PS. 2014. Innate immunity to influenza virus infection. Nat Rev Immunol 14:315–328. https://doi.org/10.1038/nri3665.
13. Garcia-Sastre A, Egorov A, Matassov D, Brandt S, Levy DE, Durbin JE, Palese P, Muster T. 1998. Influenza A virus lacking the NS1 gene replicates in interferon-deficient systems. Virology 252:324–330. https://doi.org/10.1006/viro.1998.9508.
14. Hale BG, Randall RE, Ortin J, Jackson D. 2008. The multifunctional NS1 protein of influenza A viruses. J Gen Virol 89:2359–2376. https://doi.org/10.1099/vir.0.2008/004606-0.
15. Jagger BW, Wise HM, Kash JC, Walters KA, Wills NM, Xiao YL, Dunfee RL, Schwartzman LM, Ozinsky A, Bell GL, Dalton RM, Lo A, Efstathiou S, Atkins JF, Firth AE, Taubenberger JK, Digard P. 2012. An overlapping protein-coding region in influenza A virus segment 3 modulates the host response. Science 337:199–204. https://doi.org/10.1126/science.1222213.
16. Hu J, Mo Y, Wang X, Gu M, Hu Z, Zhong L, Wu Q, Hao X, Hu S, Liu W, Liu H, Liu X, Liu X. 2015. PA-X decreases the pathogenicity of highly pathogenic H5N1 influenza A virus in avian species by inhibiting virus replication and host response. J Virol 89:4126–4142. https://doi.org/10.1128/JVI.02132-14.
17. Khaperskyy DA, McCormick C. 2015. Timing is everything: coordinated control of host shutoff by influenza A virus NS1 and PA-X proteins. J Virol 89:6528–6531. https://doi.org/10.1128/JVI.00386-15.
18. Khaperskyy DA, Schmaling S, Larkins-Ford J, McCormick C, Gaglia MM. 2016. Selective degradation of host RNA polymerase II transcripts by influenza A virus PA-X host shutoff protein. PLoS Pathog 12:e1005427. https://doi.org/10.1371/journal.ppat.1005427.
19. Oishi K, Yamayoshi S, Kawaoka Y. 2015. Mapping of a region of the PA-X protein of influenza A virus that is important for its shutoff activity. J Virol 89:8661–8665. https://doi.org/10.1128/JVI.01132-15.
20. Gao H, Sun H, Hu J, Qi L, Wang J, Xiong X, Wang Y, He Q, Lin Y, Kong W, Seng LG, Pu J, Chang KC, Liu X, Liu J, Sun Y. 2015. Twenty amino acids at the C-terminus of PA-X are associated with increased influenza A virus replication and pathogenicity. J Gen Virol 96:2036–2049. https://doi.org/10.1099/vir.0.000143.
21. Gao H, Xu G, Sun Y, Qi L, Wang J, Kong W, Sun H, Pu J, Chang KC, Liu J. 2015. PA-X is a virulence factor in avian H9N2 influenza virus. J Gen Virol 96:2587–2594. https://doi.org/10.1099/jgv.0.000232.
22. Hu J, Mo Y, Gao Z, Wang X, Gu M, Liang Y, Cheng X, Hu S, Liu W, Liu H, Chen S, Liu X, Peng D, Liu X. 2016. PA-X-associated early alleviation of the acute lung injury contributes to the attenuation of a highly pathogenic H5N1 avian influenza virus in mice. Med Microbiol Immunol 205:381–395. https://doi.org/10.1007/s00430-016-0461-2.
23. Bavagnoli L, Cucuzza S, Campanini G, Rovida F, Paolucci S, Baldanti F, Maga G. 2015. The novel influenza A virus protein PA-X and its naturally deleted variant show different enzymatic properties in comparison to the viral endonuclease PA. Nucleic Acids Res 43:9405–9417. https://doi.org/10.1093/nar/gkv926.
24. Crotta S, Davidson S, Mahlakoiv T, Desmet CJ, Buckwalter MR, Albert ML, Staeheli P, Wack A. 2013. Type I and type III interferons drive redundant amplification loops to induce a transcriptional signature in influenza-infected airway epithelia. PLoS Pathog 9:e1003773. https://doi.org/10.1371/journal.ppat.1003773.
25. DeDiego ML, Nogales A, Lambert-Emo K, Martinez-Sobrido L, Topham DJ. 2016. NS1 protein mutation I64T affects interferon responses and virulence of circulating H3N2 human influenza A viruses. J Virol 90:9693–9711. https://doi.org/10.1128/JVI.01039-16.
26. Nogales A, Martinez-Sobrido L, Topham DJ, DeDiego ML. 14 February 2017. NS1 protein amino acid changes D189N and V194I affect interferon responses, thermosensitivity and virulence of circulating H3N2 human influenza A viruses. J Virol https://doi.org/10.1128/JVI.01930-16.
27. Wolff T, Ludwig S. 2009. Influenza viruses control the vertebrate type I interferon system: factors, mechanisms, and consequences. J Interferon Cytokine Res 29:549–557. https://doi.org/10.1089/jir.2009.0066.

28. Das K, Ma LC, Xiao R, Radvansky B, Aramini J, Zhao L, Marklund J, Kuo RL, Twu KY, Arnold E, Krug RM, Montelione GT. 2008. Structural basis for suppression of a host antiviral response by influenza A virus. Proc Natl Acad Sci U S A 105:13093–13098. https://doi.org/10.1073/pnas.0805213105.
29. Kochs G, Garcia-Sastre A, Martinez-Sobrido L. 2007. Multiple anti-interferon actions of the influenza A virus NS1 protein. J Virol 81:7011–7021. https://doi.org/10.1128/JVI.02581-06.
30. Noah DL, Twu KY, Krug RM. 2003. Cellular antiviral responses against influenza A virus are countered at the posttranscriptional level by the viral NS1A protein via its binding to a cellular protein required for the 3′ end processing of cellular pre-mRNAS. Virology 307:386–395. https://doi.org/10.1016/S0042-6822(02)00127-7.
31. Ayllon J, Domingues P, Rajsbaum R, Miorin L, Schmolke M, Hale BG, Garcia-Sastre A. 2014. A single amino acid substitution in the novel H7N9 influenza A virus NS1 protein increases CPSF30 binding and virulence. J Virol 88:12146–12151. https://doi.org/10.1128/JVI.01567-14.
32. Nemeroff ME, Barabino SM, Li Y, Keller W, Krug RM. 1998. Influenza virus NS1 protein interacts with the cellular 30 kDa subunit of CPSF and inhibits 3′end formation of cellular pre-mRNAs. Mol Cell 1:991–1000. https://doi.org/10.1016/S1097-2765(00)80099-4.
33. Twu KY, Noah DL, Rao P, Kuo RL, Krug RM. 2006. The CPSF30 binding site on the NS1A protein of influenza A virus is a potential antiviral target. J Virol 80:3957–3965. https://doi.org/10.1128/JVI.80.8.3957-3965.2006.
34. Hale BG, Steel J, Medina RA, Manicassamy B, Ye J, Hickman D, Hai R, Schmolke M, Lowen AC, Perez DR, Garcia-Sastre A. 2010. Inefficient control of host gene expression by the 2009 pandemic H1N1 influenza A virus NS1 protein. J Virol 84:6909–6922. https://doi.org/10.1128/JVI.00081-10.
35. Lee J, Yu H, Li Y, Ma J, Lang Y, Duff M, Henningson J, Liu Q, Li Y, Nagy A, Bawa B, Li Z, Tong G, Richt JA, Ma W. 2017. Impacts of different expressions of PA-X protein on 2009 pandemic H1N1 virus replication, pathogenicity and host immune responses. Virology 504:25–35. https://doi.org/10.1016/j.virol.2017.01.015.
36. Louie JK, Jean C, Acosta M, Samuel MC, Matyas BT, Schechter R. 2011. A review of adult mortality due to 2009 pandemic (H1N1) influenza A in California. PLoS One 6:e18221. https://doi.org/10.1371/journal.pone.0018221.
37. Seibert CW, Kaminski M, Philipp J, Rubbenstroth D, Albrecht RA, Schwalm F, Stertz S, Medina RA, Kochs G, Garcia-Sastre A, Staeheli P, Palese P. 2010. Oseltamivir-resistant variants of the 2009 pandemic H1N1 influenza A virus are not attenuated in the guinea pig and ferret transmission models. J Virol 84:11219–11226. https://doi.org/10.1128/JVI.01424-10.
38. Simonsen L, Spreeuwenberg P, Lustig R, Taylor RJ, Fleming DM, Kroneman M, Van Kerkhove MD, Mounts AW, Paget WJ, Teams GLC. 2013. Global mortality estimates for the 2009 influenza pandemic from the GLaMOR project: a modeling study. Plos Med 10:e1001558. https://doi.org/10.1371/journal.pmed.1001558.
39. Nogales A, Martinez-Sobrido L. 22 December 2016. Reverse genetics approaches for the development of influenza vaccines. Int J Mol Sci https://doi.org/10.3390/ijms18010020.
40. Grohskopf LA, Sokolow LZ, Broder KR, Olsen SJ, Karron RA, Jernigan DB, Bresee JS. 2016. Prevention and control of seasonal influenza with vaccines. MMWR Recomm Rep 65:1–54. https://doi.org/10.15585/mmwr.rr6505a1.
41. Principi N, Esposito S. 2017. Protection of children against influenza: emerging problems. Hum Vaccines Immunother 2017:1–8. https://doi.org/10.1080/21645515.2017.1279772.
42. Feng KH, Sun M, Iketani S, Holmes EC, Parrish CR. 2016. Comparing the functions of equine and canine influenza H3N8 virus PA-X proteins: suppression of reporter gene expression and modulation of global host gene expression. Virology 496:138–146. https://doi.org/10.1016/j.virol.2016.06.001.
43. Gao H, Sun Y, Hu J, Qi L, Wang J, Xiong X, Wang Y, He Q, Lin Y, Kong W, Seng LG, Sun H, Pu J, Chang KC, Liu X, Liu J. 2015. The contribution of PA-X to the virulence of pandemic 2009 H1N1 and highly pathogenic H5N1 avian influenza viruses. Sci Rep 5:8262. https://doi.org/10.1038/srep08262.
44. Geiss GK, Salvatore M, Tumpey TM, Carter VS, Wang X, Basler CF, Taubenberger JK, Bumgarner RE, Palese P, Katze MG, Garcia-Sastre A. 2002. Cellular transcriptional profiling in influenza A virus-infected lung epithelial cells: the role of the nonstructural NS1 protein in the evasion of the host innate defense and its potential contribution to pandemic influenza. Proc Natl Acad Sci U S A 99:10736–10741. https://doi.org/10.1073/pnas.112338099.
45. Konig R, Stertz S, Zhou Y, Inoue A, Hoffmann HH, Bhattacharyya S, Alamares JG, Tscherne DM, Ortigoza MB, Liang Y, Gao Q, Andrews SE, Bandyopadhyay S, De Jesus P, Tu BP, Pache L, Shih C, Orth A, Bonamy G, Miraglia L, Ideker T, Garcia-Sastre A, Young JA, Palese P, Shaw ML, Chanda SK. 2010. Human host factors required for influenza virus replication. Nature 463:813–817. https://doi.org/10.1038/nature08699.
46. Dove BK, Surtees R, Bean TJ, Munday D, Wise HM, Digard P, Carroll MW, Ajuh P, Barr JN, Hiscox JA. 2012. A quantitative proteomic analysis of lung epithelial (A549) cells infected with 2009 pandemic influenza A virus using stable isotope labelling with amino acids in cell culture. Proteomics 12:1431–1436. https://doi.org/10.1002/pmic.201100470.
47. Sutejo R, Yeo DS, Myaing MZ, Hui C, Xia J, Ko D, Cheung PC, Tan BH, Sugrue RJ. 2012. Activation of type I and III interferon signalling pathways occurs in lung epithelial cells infected with low pathogenic avian influenza viruses. PLoS One 7:e33732. https://doi.org/10.1371/journal.pone.0033732.
48. Hai R, Martinez-Sobrido L, Fraser KA, Ayllon J, Garcia-Sastre A, Palese P. 2008. Influenza B virus NS1-truncated mutants: live-attenuated vaccine approach. J Virol 82:10580–10590. https://doi.org/10.1128/JVI.01213-08.
49. Nogales A, Baker SF, Ortiz-Riano E, Dewhurst S, Topham DJ, Martinez-Sobrido L. 2014. Influenza A virus attenuation by codon deoptimization of the NS gene for vaccine development. J Virol 88:10525–10540. https://doi.org/10.1128/JVI.01565-14.
50. Martinez-Sobrido L, Emonet S, Giannakas P, Cubitt B, Garcia-Sastre A, de la Torre JC. 2009. Identification of amino acid residues critical for the anti-interferon activity of the nucleoprotein of the prototypic arenavirus lymphocytic choriomeningitis virus. J Virol 83:11330–11340. https://doi.org/10.1128/JVI.00763-09.
51. Martinez-Sobrido L, Zuniga EI, Rosario D, Garcia-Sastre A, de la Torre JC. 2006. Inhibition of the type I interferon response by the nucleoprotein of the prototypic arenavirus lymphocytic choriomeningitis virus. J Virol 80:9192–9199. https://doi.org/10.1128/JVI.00555-06.
52. Reed LJ, Muench H. 1938. A simple method of estimating fifty percent endpoints. Am J Hyg 27:493–497.
53. Tavares LP, Teixeira MM, Garcia CC. 2017. The inflammatory response triggered by Influenza virus: a two edged sword. Inflamm Res 66:283–302. https://doi.org/10.1007/s00011-016-0996-0.
54. Wang Z, Loh L, Kedzierski L, Kedzierska K. 2016. Avian influenza viruses, inflammation, and CD8(+) T cell immunity. Front Immunol 7:60. https://doi.org/10.3389/fimmu.2016.00060.
55. Baker SF, Guo H, Albrecht RA, Garcia-Sastre A, Topham DJ, Martinez-Sobrido L. 2013. Protection against lethal influenza with a viral mimic. J Virol 87:8591–8605. https://doi.org/10.1128/JVI.01081-13.
56. Tripathi S, Batra J, Lal SK. 2015. Interplay between influenza A virus and host factors: targets for antiviral intervention. Arch Virol 160:1877–1891. https://doi.org/10.1007/s00705-015-2452-9.
57. Watanabe T, Kawaoka Y. 2015. Influenza virus-host interactomes as a basis for antiviral drug development. Curr Opin Virol 14:71–78. https://doi.org/10.1016/j.coviro.2015.08.008.
58. Hai R, Schmolke M, Varga ZT, Manicassamy B, Wang TT, Belser JA, Pearce MB, Garcia-Sastre A, Tumpey TM, Palese P. 2010. PB1-F2 expression by the 2009 pandemic H1N1 influenza virus has minimal impact on virulence in animal models. J Virol 84:4442–4450. https://doi.org/10.1128/JVI.02717-09.
59. Martinez-Sobrido L, Garcia-Sastre A. 3 August 2010. Generation of recombinant influenza virus from plasmid DNA. J Vis Exp https://doi.org/10.3791/2057.
60. Park MS, Shaw ML, Munoz-Jordan J, Cros JF, Nakaya T, Bouvier N, Palese P, Garcia-Sastre A, Basler CF. 2003. Newcastle disease virus (NDV)-based assay demonstrates interferon-antagonist activity for the NDV V protein and the Nipah virus V, W, and C proteins. J Virol 77:1501–1511. https://doi.org/10.1128/JVI.77.2.1501-1511.2003.
61. Quinlivan M, Zamarin D, Garcia-Sastre A, Cullinane A, Chambers T, Palese P. 2005. Attenuation of equine influenza viruses through truncations of the NS1 protein. J Virol 79:8431–8439. https://doi.org/10.1128/JVI.79.13.8431-8439.2005.
62. Baker SF, Nogales A, Finch C, Tuffy KM, Domm W, Perez DR, Topham DJ, Martinez-Sobrido L. 2014. Influenza A and B virus intertypic reassortment through compatible viral packaging signals. J Virol 88:10778–10791. https://doi.org/10.1128/JVI.01440-14.
63. Nogales A, Baker SF, Martinez-Sobrido L. 2014. Replication-competent

influenza A viruses expressing a red fluorescent protein. Virology 476C: 206–216.
64. Capul AA, de la Torre JC. 2008. A cell-based luciferase assay amenable to high-throughput screening of inhibitors of arenavirus budding. Virology 382:107–114. https://doi.org/10.1016/j.virol.2008.09.008.
65. Cheng BY, Ortiz-Riano E, Nogales A, de la Torre JC, Martinez-Sobrido L. 2015. Development of live-attenuated arenavirus vaccines based on codon deoptimization. J Virol 89:3523–3533. https://doi.org/10.1128/JVI.03401-14.
66. Nakajima Y, Kobayashi K, Yamagishi K, Enomoto T, Ohmiya Y. 2004. cDNA cloning and characterization of a secreted luciferase from the luminous Japanese ostracod, Cypridina noctiluca. Biosci Biotechnol Biochem 68:565–570. https://doi.org/10.1271/bbb.68.565.
67. Solorzano A, Webby RJ, Lager KM, Janke BH, Garcia-Sastre A, Richt JA. 2005. Mutations in the NS1 protein of swine influenza virus impair anti-interferon activity and confer attenuation in pigs. J Virol 79: 7535–7543. https://doi.org/10.1128/JVI.79.12.7535-7543.2005.
68. Nogales A, Rodriguez-Sanchez I, Monte K, Lenschow DJ, Perez DR, Martinez-Sobrido L. 2016. Replication-competent fluorescent-expressing influenza B virus. Virus Res 213:69–81. https://doi.org/10.1016/j.virusres.2015.11.014.
69. National Research Council. 2011. Guide for the care and use of laboratory animals, 8th ed. National Academies Press, Washington, DC.
70. Livak KJ, Schmittgen TD. 2001. Analysis of relative gene expression data using real-time quantitative PCR and the 2(−Delta Delta C(T)) method. Methods 25:402–408. https://doi.org/10.1006/meth.2001.1262.